

Multichannel Seismic Evidence for a Subcrustal Intrusive Complex Under Oahu and a Model for Hawaiian Volcanism

URI S. TEN BRINK¹

Lamont-Doherty Geological Observatory and Department of Geological Sciences, Columbia University, Palisades, New York

THOMAS M. BROCHER

U.S. Geological Survey, Menlo Park, California

Coincident multichannel seismic reflection and refraction data acquired during a wide-aperture two-ship experiment provide evidence for a complex crust-mantle (C-M) transition under Oahu, Hawaii. Several large-aperture common depth point lines and three expanding spread profiles suggest the existence of an anomalously thick (3–6 km) C-M transition zone underneath the volcanic ridge which extends for distances of 100 km to the north and south from the center of Oahu. The anomalous C-M transition may represent a plutonic complex which intruded into the upper mantle and the lower crust in a 200-km-wide area centered at Oahu. The existence of such a large volume of intrusions near the base of the crust implies that the surficial expression of volcanism constitutes only a small fraction of the amount of melt generated at depth under the Hawaiian Islands. This interpretation is in accord with previous petrological models which predict trapping and accumulation of upwelling magma at and below the Moho. We have constructed a model which suggests that the interaction between the upwelling magma and the lithospheric flexural stress field may modulate the characteristic eruption history of Hawaiian volcanoes. In particular, the model for the plane stress field which accompanies the flexure of the oceanic crust around island chains indicates that the stress field under individual volcanoes varies considerably with its position relative to the tip of the chain. As a Hawaiian-sized volcano develops, the magnitude of deviatoric compressive stresses under it is probably sufficient to block the conduits of the upwelling magma within the oceanic crust and to terminate eruptions. Further upwelling magma is predicted by the models to be ponded at the base of the crust. Resumption of posterosional volcanism seems to occur at a constant distance behind the center of active shield volcanism, as the horizontal compressive stresses along the axis of the chain are released. Observed orientations of dikes of this volcanic phase agree with the directions of the maximum calculated stresses. Our model implies that magma upwells over a 300-km-wide zone and that the oceanic plate may not be fractured under the islands.

1. INTRODUCTION

According to the "hot spot" hypothesis, the Hawaiian Island chain was formed by the motion of the Pacific plate over a melting anomaly in the asthenosphere [Wilson, 1963] produced by rising thermal plumes from the lower mantle [Morgan, 1972]. Studies of the free air gravity field around the Hawaiian Islands show that gravity data are consistent with flexural models in which the islands represent a surface load emplaced on the top of the lithosphere, which responds in a manner similar to an elastic plate overlying a weak substratum [Walcott, 1970; Watts and Cochran, 1974; Watts, 1978].

Hawaiian volcanoes undergo four volcanic stages with distinct compositions of lavas and xenoliths. The stages (depicted in Figure 1) are (1) submarine eruption of alkalic and tholeiitic basalt, (2) tholeiitic shield volcano building, (3) postcaldera collapse which caps the shield with alkali basalts, and, after a period of quiescence and erosion, (4) posterosional eruptions of alkali basalt, basanite, nephelinite, and melilite. The xenolith assemblages differ at each eruptive stage and may represent differences in the depth of source and/or the magma

chamber [Clague, 1987]. The eruption rate (Figure 1) varies considerably between stages, dropping by 2 orders of magnitude or more within 0.1–0.2 m.y. of the end of the shield-building stage, and is followed by a period of quiescence [Clague, 1987; Clague and Dalrymple, 1987].

Few explanations for the resumption of volcanism at the posterosional stage, after a long period of quiescence (as much as 2.5 m.y.), have been proposed [Jackson and Wright, 1970; Gurriet, 1987; Nakamura and Fujii, 1987]. Particularly intriguing has been the suggestion that the posterosional volcanic stage occurs at the nearly constant distance of 190 ± 30 km from the contemporaneous active shield volcanism, regardless of the significant changes in propagation rate of the Hawaiian chain [Clague and Dalrymple, 1987].

We present new results bearing on these observations using data from a two-ship multichannel seismic experiment performed in 1982 near Oahu (Figure 2) by the Lamont-Doherty Geological Observatory and the Hawaii Institute of Geophysics. The experiment was designed to constrain models for the flexural deformation of the oceanic crust due to the volcanic load of the Hawaiian ridge by determining detailed seismic velocities and mapping the lateral extent of sedimentary and crustal reflections. This paper focuses on the abnormal crust-mantle (C-M) transition under the flexural moats and volcanic ridge near Oahu that we interpret as "underplating" of the oceanic crust by a plutonic complex. We present evidence favoring the hypothesis that the development of both the lower crustal plutonic complex and the posterosional eruptions may originate in the interaction between the volcanism

¹ Now at Department of Geophysics, Stanford University, Stanford, California.

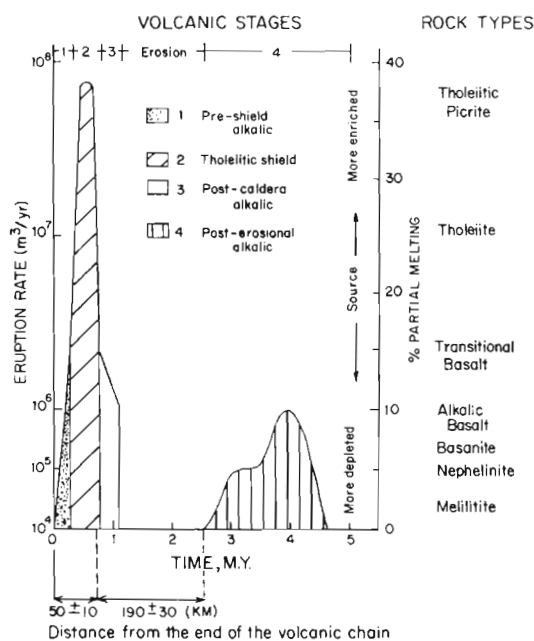


Fig. 1. Eruption rates and percent partial melting during the evolutionary stages of a hypothetical Hawaiian volcano (modified from the work by Clague [1987]). The posterosional eruptions follow a period of erosion and quiescence of variable duration (0.4–2.5 m.y.) but occur at a constant distance from the shield [Clague and Dalrymple, 1987]. Many of the Hawaiian volcanoes are separated by 50 ± 10 km from each other, suggesting that a constant distance is also maintained between the preshield (nascent) and the shield stages.

associated with the hot spot and the local stress field which accompanies the flexure.

We begin in section 2 by describing the acquisition and processing methods of the seismic data with emphasis on the large-aperture expanding spread profile (ESP) data. In section 3 we present the seismic results and compare them to other studies of volcanic islands and seamounts and to aseismic ridges. In section 4 we cite the reasons for the interpretation of the anomalous C-M transition as a subcrustal plutonic complex. In section 5 we present a semiquantitative model for the stress field under the Hawaiian Island chain which suggests that pluton formation is an integral part of the characteristic volcanic and magmatic history of linear volcanic chains. A discussion of the model, its predictions for the nature of the lithosphere and the hot spot under Hawaii completes the paper. Throughout the paper the widely accepted means of referring to thicknesses and depths in terms of two-way travel time (TWTT) will be used, where the dimension is seconds.

2. DATA ACQUISITION AND SEISMIC PROCESSING

The extensive data set reported in this study includes multi-channel seismic refraction profiles (ESPs) and coincident and crossing large-aperture multichannel reflection profiles. A detailed description of these acquisition and processing methods can be found in the works by Stoffa and Buhl [1979], Buhl *et al.* [1982], and NAT Study Group [1985]. Details of the navigation, timing and range errors, and range corrections for the Hawaiian experiment are given by ten Brink [1986].

Data Acquisition

A total of four expanding spread profiles with maximum source-receiver offsets ranging between 60 and 95 km were

collected on the volcanic ridge between Oahu and Molokai and on the flexural moats to the north and south of Oahu (Figure 2). Each ESP was obtained using a three-element air gun array totaling 32 L (1932 cubic inches) and 27.2- and 81.6-kg (60- and 180-lb) ammonium nitrate explosive charges. The structure under each ESP was constrained by standard aperture (3.6 km) common depth point (CDP) reflection profiles collected along one half of each ESP and large-aperture (7.2 km) CDP profiles on the other half using three-element air gun arrays totaling 32 and 40 L (1932 and 2466 cubic inches). The center frequencies for the two sizes of air guns in the ships' arrays were 6 and 8 Hz, respectively (P. Buhl, personal communication, 1985). For the experiment the R/V *Conrad* was equipped with a 3.6-km-long multichannel array consisting of 48 hydrophone groups, with an average group spacing of 75 m. Large-aperture CDP profiles were also collected along long lines perpendicular to the ESPs and passing through their midpoints (Figure 2). On the volcanic ridge, both standard and large-aperture CDP profiles were collected parallel to the ESPs.

Processing CDP Profiles

CDP data processing included prestack velocity filtering to remove multiples in shallow water (line 330) and scattered noise in deep water (lines 301 and 332). Large-aperture CDP data (0.3–7.5 km), obtained by combining standard (0.3–3.9 km) and wide-aperture (3.9–7.5 km) CDP records, generally exhibited greatly enhanced deep reflectors in the moat and the arch and in some cases revealed reflectors that were not visible in the standard aperture CDP data (compare Figures 3a and 3b). The profiles presented here are unmigrated because the reflectors of interest along the C-M boundary are all subhorizontal and would not migrate an appreciable distance. This assumption was verified by performing line segment migration (not shown) on one of the profiles (line 310) and comparing it to the unmigrated section. More detailed aspects of the processing of wide-aperture records can be found in the work by ten Brink [1986].

Processing and Interpretation Procedures for the Expanding Spread Profiles

Processing of the ESPs included collecting the traces in range bins 100 m wide and summing all traces within each bin along a ray parameter of 0.125 s/km, giving a nominal signal-to-noise ratio enhancement of 4 to the air gun ESPs. ESPs acquired using explosive sources were processed separately from those collected with air gun sources except that the air gun data were used to interpolate arrivals on the explosive profiles to smaller ranges.

The interpretation of the ESPs assumed laterally homogeneous layers. This assumption is justified by the nearly flat seafloor and subbottom topography along the coincident CDP lines. The validity of this assumption was checked for ESP 5 collected over the volcanic ridge where the subbottom structure is the most heterogeneous within the study area. Insignificant differences were found between our velocity-depth solution and that derived from iterative two-dimensional synthetic seismogram modeling [Lindwall and Brocher, 1986]. Furthermore, the geometry of moving source and receiver tends to average out small lateral variations in the velocity structure [Diebold and Stoffa, 1981]. The large fold of 16–17 traces stacked into a single trace in the air gun

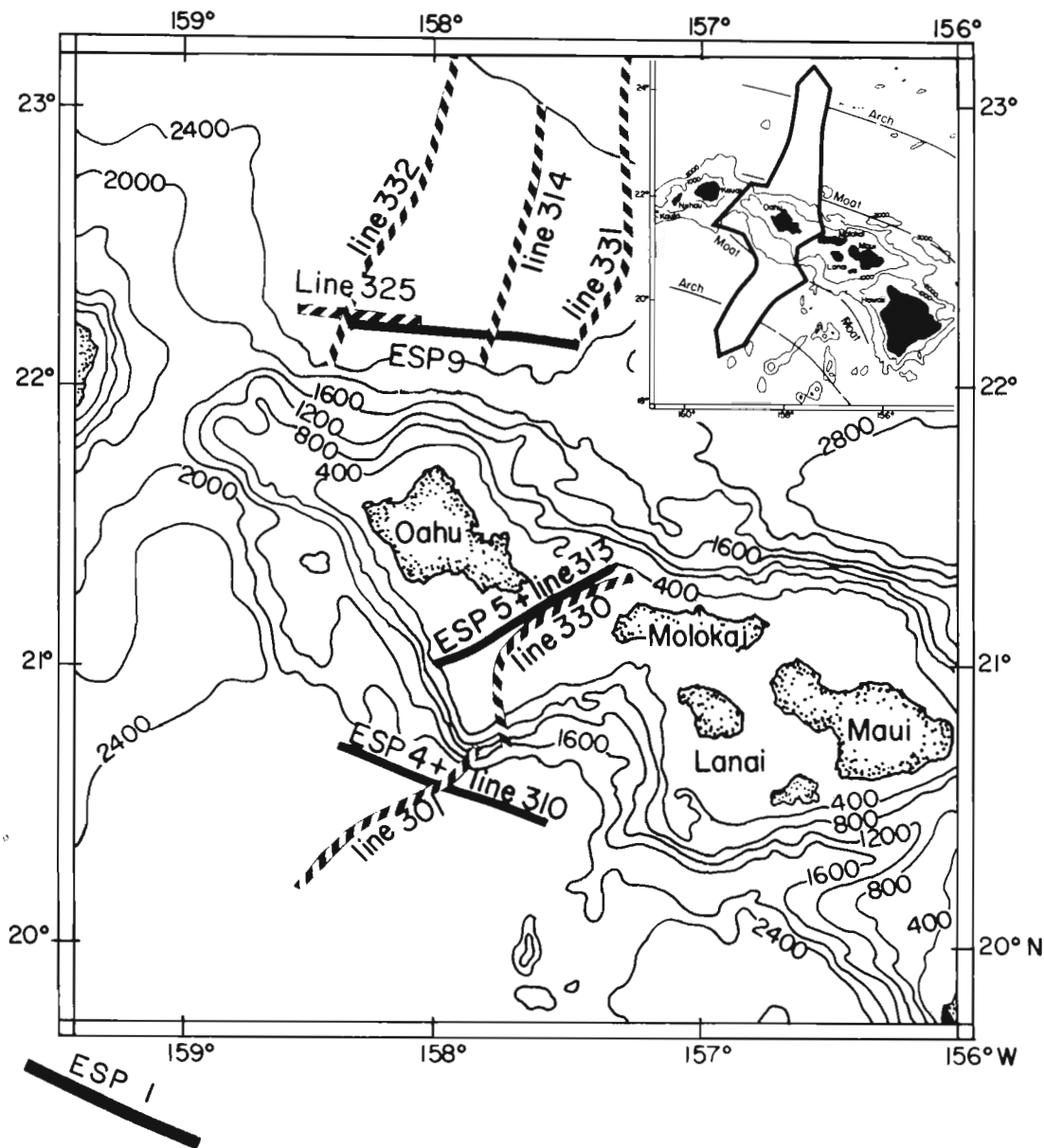


Fig. 2. Location map of the CDP profiles (dotted lines) and ESP profiles (solid lines) discussed in this paper. Bathymetry is contoured at 400-fathom intervals (1 fathom = 1.8288 m) and is based on the work by Chase *et al.* [1970]. The inset shows the study area of our two-ship multichannel seismic experiment (enclosed by a heavy line) which comprised a 600-km-long traverse across the flexural arches and moats (dashed lines) and the volcanic ridge around Oahu.

ESPs also averages out topographic variations on the scale of the receiver array length (3.6 km).

The procedure used to obtain velocity-depth solutions included τ - p analysis and iterative ray tracing of travel times and comparison of relative amplitudes with WKBJ synthetic seismograms. Transformation of the data to the τ - p (intercept time-ray parameter) domain was carried out by automatic slowness stacking along overlapping subarrays of source-receiver offsets [Stoffa *et al.*, 1981]. Digitized τ - p curves were inverted by the recursive τ sum method [Diebold and Stoffa, 1981], and the resultant solutions were improved by iteratively tracing rays through the model. The estimated error of the travel time fits to the observed curves was usually $\frac{1}{4}$ – $\frac{1}{3}$ of the wavelength (about 25 ms) or better. Important constraints on the solutions were obtained from the vertical TWT of reflections in CDP lines, collected along the ESPs and crossing their midpoints (Table 1). Although extremal bounds were

not placed on the solutions, we did investigate radically different solutions that would alter the interpretation of the ESPs.

Synthetic seismograms were calculated using WKBJ theory described by Chapman [1978]. This modeling places additional constraints on the velocity-depth solutions and, in particular, was used to investigate the thickness and nature of the anomalous crust-mantle transition. Precritical reflections from the top and bottom of the crust-mantle transition zone were included in the synthetics since they were observed on the CDP records.

3. SEISMIC EVIDENCE FOR AN ANOMALOUS CRUST-MANTLE TRANSITION

Both the CDP and ESP data provide evidence for an anomalous C-M transition near Oahu. Large-aperture CDP profiles (0.30–7.5 km) in the flexural moat north and south of Oahu show a complex crust-mantle (C-M) transition including len-

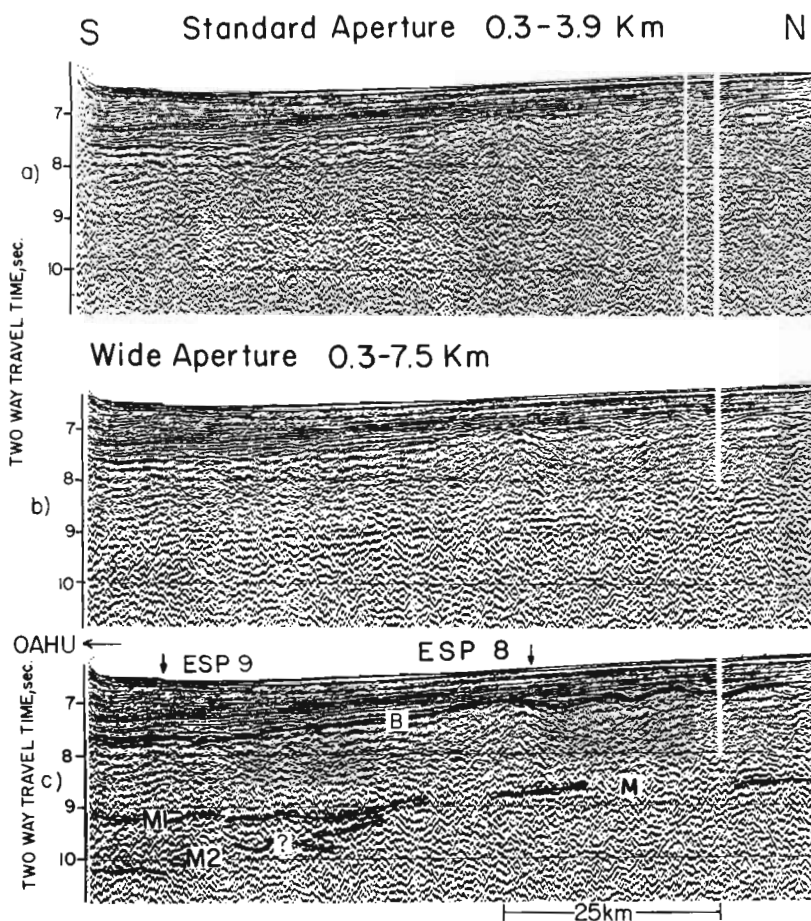


Fig. 3. CDP line 314, located north of Oahu and oriented perpendicular to the island chain (Figure 2). (a) Standard aperture (0.3–3.9 km) CDP profile in which the lower crustal reflections are band-pass filtered between 6 and 15 Hz. (b) Same CDP profile with combined standard and large-aperture CDP gathers (0.3–7.5 km) in which the lower crustal reflections are band-pass filtered between 4 and 10 Hz. (c) Interpretation of Figure 3b. Note that deep reflections (M1) are more clearly seen on the large-aperture CDP profile (Figure 3b) than on the standard aperture CDP profile (Figure 3a). The crust above M1 thins progressively toward Oahu.

ticular bodies, thinning and thickening of the crustal section, and unusually high topography of the Moho reflection, unlike the simple Moho reflections seen under the flexural arch (U. S. ten Brink and T. M. Brocher, Multichannel seismic evidence for variations in crustal thickness across the Molokai Fracture Zone in the mid-Pacific, submitted to *Journal of Geophysical Research*, 1987 (hereinafter tBB, 1987)). This anomalous C-M transition constitutes the main evidence for the existence of a subcrustal plutonic complex near Oahu. The ESP data suggest that the C-M transition also has anomalous thickness and velocity under Oahu.

Large-Aperture CDP Profiles

Several large-aperture CDP profiles collected north of Oahu (Figure 2) show two intermittent reflections (M1 and M2) at the base of the crust. On line 314 at a distance of 40 km from the southern end of the line the Moho reflection (M) bifurcates (Figure 3). The M1 reflection flattens (at a depth of 9.1 s) while the sediment-crust interface deepens to the south, resulting in a thinning of the igneous crust by approximately 0.5 s. A weaker M2 reflection dips southward to a depth of 10.2 s. On line 325 these reflectors appear to delineate a lenticular body almost 1 s thick (Figure 4). The crustal thickness

(in TWTT) over the lens-shaped body is 0.3 s thinner than that of normal oceanic crust in the area and the igneous basement (B) shoals eastward, causing a thinning of the overlying sedimentary section by 0.15–0.2 s. This lenticular body seems to have uplifted the overlying crust, causing a gentle tilting of the top of the crust. The TWTTs to reflections M1 and M2 are similar to the TWTT to these reflections on cross lines 314 and 332. This observation and the nearly horizontal seafloor topography indicate that the reflections M1 and M2 are probably real lower crustal events and are not artifacts caused by a shallow-ridge-parallel structure. The M2 reflection and thinning of the igneous crust are also present, although observed less clearly, in line 331 [Watts *et al.*, 1985, Figure 2] and line 332 (not shown here).

Large-aperture CDP lines 301 (Figure 5) and 310, recorded south of Oahu (Figure 2), also show two or more reflections from the base of the crust. On line 310 a reflection (M, at 9 s TWTT) at the west end of the profile dips eastward toward the midpoint of ESP 4, where it is distinguished by rugged structural relief and multiple reflections (M2) possibly extending as deep as 10.8 s. Although the sediment-crust interface is not well resolved, the total crustal thickness along line 310 appears to vary from an unusually large thickness (greater

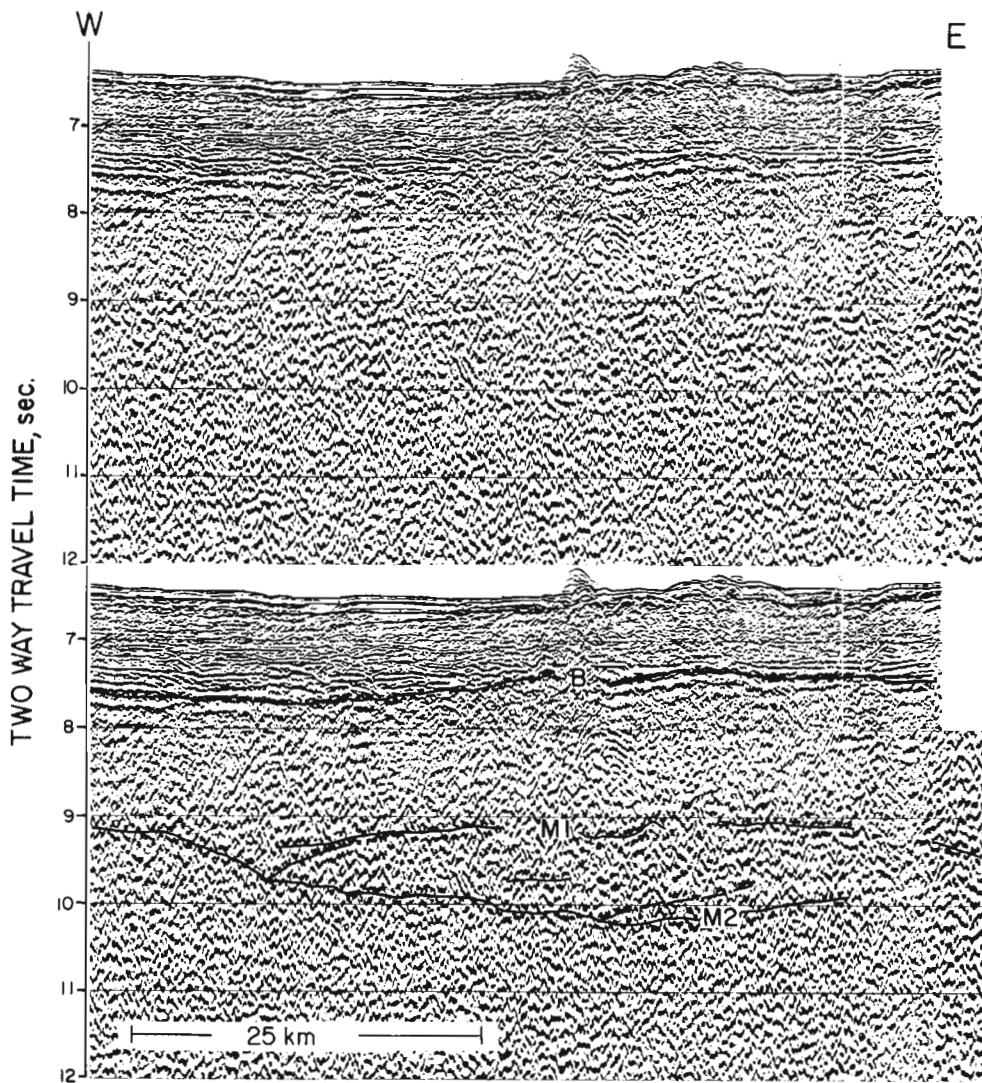


Fig. 4. Uninterpreted (top) and interpreted (bottom) large-aperture (0.3–7.5 km) CDP line 325, showing a set of reflections, M1 and M2, bounding a lenticular shape at the crust-mantle interface. The crust above reflector M1 is unusually thin, and reflection B, marking the top of the oceanic crust, is domed upward above the lenticular shape.

(than 2.5 s) to a normal oceanic crustal thickness of 2 s at the east end of the line (tBB, 1987). On line 301, reflections M1 and M2 are composed of short segments (5–20 km long) arranged as downgoing steps offset 0.1–0.4 s toward the island (Figure 5); the total crustal thickness to M2 is about 2.5 s.

Several lines of evidence lead us to believe that the M1 and M2 reflections are legitimate in-the-plane lower crustal/upper mantle events. The frequency contents of these reflections are typical for those of the lower crust and upper mantle and atypical for the seafloor and multiples of the seafloor. These reflections are not predominantly water column arrivals because they stack better at velocities appropriate for the lower crust than at water and sediment velocities. Although Tsai [1984] shows that the rough basaltic basement can generate scattered noise with artificially high stacking velocities, pre-stack velocity filtering of lines 301 and 332 confirmed that the deep crustal reflections have primary stacking velocities. The lateral continuity of the reflections observed in lines of different orientations precludes the possibility that these reflectors are located out of the plane of the profiles ("sideswipes"). In particular, buried linear basement escarpments are unlikely

sources for these reflections because the orientation of the CDP lines is oblique to the direction of plate propagation (i.e., the plate's "flow lines").

Crust-Mantle Structure Under the Flexural Moat

The two ESPs (4 and 9) collected in the flexural moat north and south of Oahu (Figure 2) provided additional evidence for an anomalous thickening of the C-M transition zone. ESPs 4 and 9 are compared to ESP 1, located on normal oceanic crust south of Oahu, in Figure 6. Velocity-depth solutions obtained through τ sum inversion and forward modeling of the travel times provide nearly identical estimates of the total crustal thickness, depth to the top of the C-M transition, and hence thickness of the C-M transition (Figure 7; Table 1). WKBJ synthetic seismograms document that the velocity gradients in these thick C-M transition zones strongly focus returning energy into narrow range windows. These WKBJ synthetic seismograms support an anomalous C-M transition thickness for ESP 9 (Figure 8). Synthetic seismograms calculated for the thick C-M transition of ESP 4 predict a much

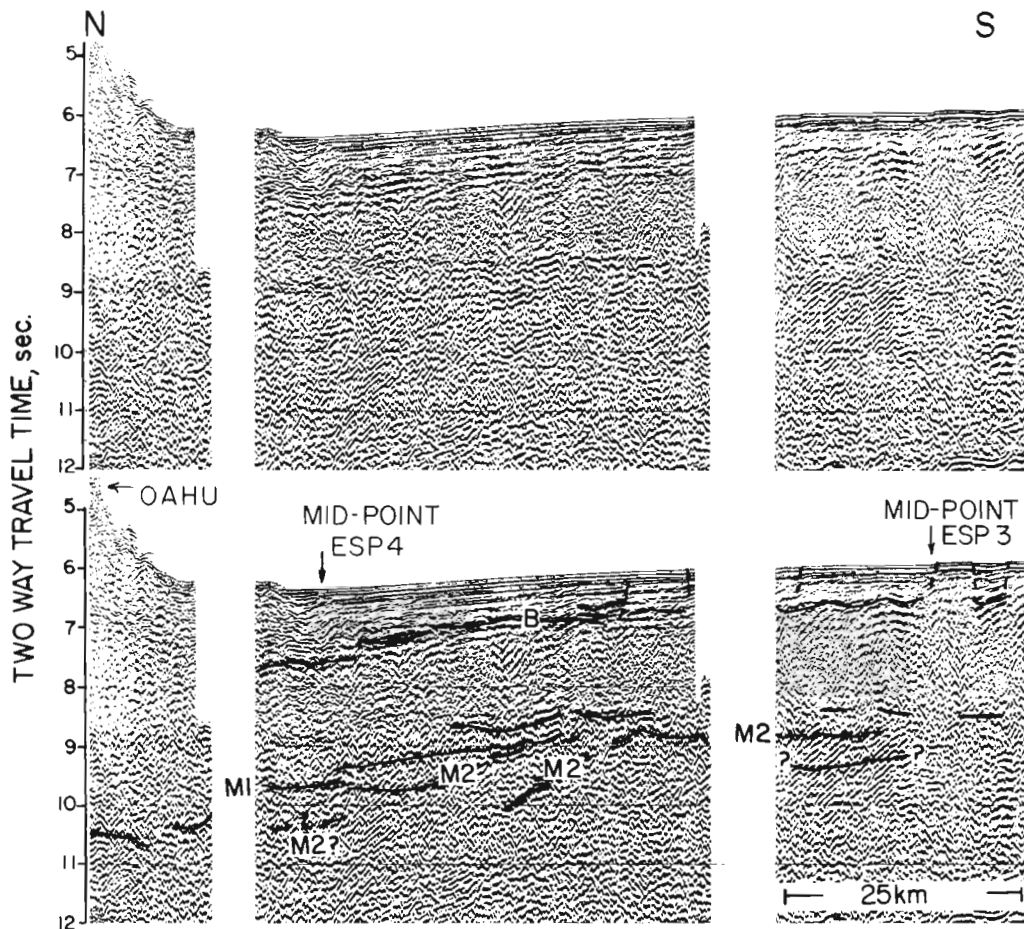


Fig. 5. Uninterpreted (top) and interpreted (bottom) large-aperture CDP (0.3–7.5 km) line 301, which traverses the flexural moat south of Oahu (Figure 2). Dashed lines mark possible faults. Note the intermittent character of the M1 and M2 reflections.

narrower amplitude range distribution (34–55 km) for the *PmP* arrival than is observed in Figure 6 (23–55 km). Although the observed amplitude range distribution on ESP 4 is better fit with a thin (roughly 1 km) C-M transition zone, the travel times predicted by this model for the *PmP* branch at ranges of 45–55 km do not match the observed phase velocity of this arrival.

The ESP solutions having a thick C-M transition explain the M2 reflections observed on the crossing CDP profiles for ESPs 4 and 9 (Figures 3 and 5) as reflections from the base of the C-M transition. The solutions obtained from the amplitude modeling of ESP 4 suggest that some of the M2 reflections could be explained as events originating in the upper mantle.

Crust-Mantle Structure Under the Volcanic Ridge

The C-M transition under the volcanic ridge was investigated using ESP 5 and two CDP profiles, lines 330 and 313 (Figure 2), collected over the volcanic ridge between Oahu and Molokai in the relatively flat and shallow (average of 0.8 s deep) seafloor of the Kaiwi channel (Figure 2). The interpreted shallow structure from these profiles includes a basin 3–4 km thick which abuts against a rift zone to the NE. Below the

basin a volcanic edifice over 5 km thick rests on what may represent unaltered oceanic layer 3.

Our interpretation of ESP 5 was strongly guided by two sets of lower crustal reflections (at 4.1–4.5 s and 7.0–7.3 s) identified on CDP line 330 (Figure 9a) which suggest (from a depth conversion of the CDP line) a gently dipping structure NE toward the rift zone. We infer that these reflections are not water or sediment column multiples since their travel times do not mimic those of earlier arrivals and they survived prestack velocity filtering which progressively passed higher stacking velocities with depth. The more coherent of these reflections, at 7.0–7.3 s, is also found in an adjacent CDP line, 313, at similar TWTT.

Although ESP 5 (Figure 9b) differs markedly from other ESPs around Oahu in its unusually thick volcanic and crustal section, being characterized by several branches with discrete phase velocities, our discussion of this record focuses only on the lower crustal section. Below the first arrival, B3, having a phase velocity of 7.1 km/s, two second arrivals, B4 and B5, are also distinguishable (Figure 9b). The absence of a *Pn* branch and the abrupt change in phase velocity of B4 and B5 beyond the 54-km range are attributed to subbasement topography [Lindwall and Brocher, 1986].

The B3 branch (Figure 9b) is modeled as a reflection from

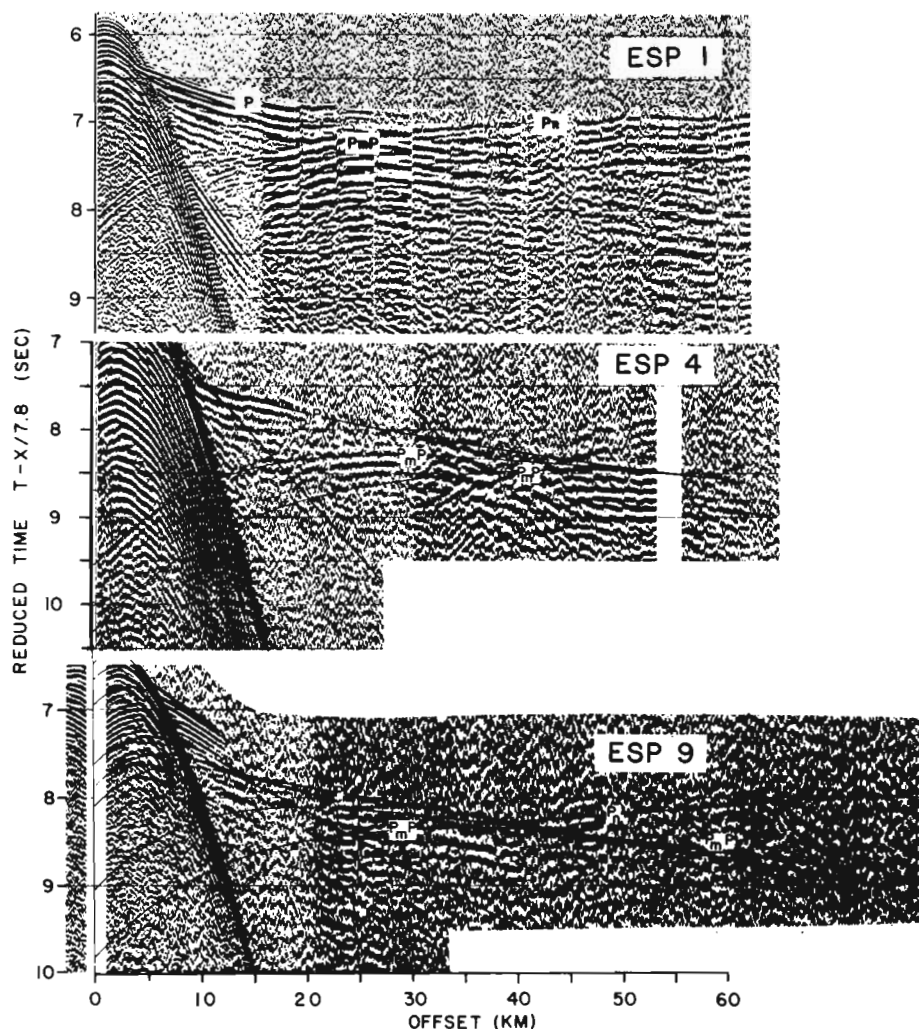


Fig. 6. The records obtained using explosive sources for ESPs 1, 4, and 9 plotted with reduced travel times using 7.8 km/s. ESPs 4 and 9 are located in the flexural moats north and south of the island (Figure 2) and exhibit atypical upper mantle reflections (PmP) and refractions (Pn) indicative of an unusually thick (2–3 km) crust-mantle transition zone. ESP 1, located in the flexural arch south of Oahu (Figure 2), is representative of a normal oceanic crustal structure. The data are plotted in true relative amplitude with no correction for geometrical spreading.

the bottom of a 3.3-km-thick layer of 6.8- to 7.0-km/s material (Table 1). The vertical TWTT to the top of this layer is modeled as corresponding to the reflection seen on CDP line 330 at 4.1–4.5 s. The velocity and thickness of this layer are compatible with those observed in layer 3 in ESPs north of the island [Watts *et al.*, 1985; tBB, 1987], suggesting that oceanic layer 3 may be continuous under the volcanic ridge. P wave velocities for this layer seem to rule out the possibility that it is part of the volcanic edifice even when the appropriate pressures are considered [Manghnani and Woollard, 1968]. The τ sum solutions (Figure 7) and an alternative ray-tracing solution suggest that not only layer 3 but also the layer 2/layer 3 transition may be preserved under the volcanic ridge. On the basis of the above solutions, the top of the oceanic crust under the volcanic ridge lies at a depth range between 7.5 and 9.5 km.

The WKB synthetic seismograms indicate that the B4 and B5 branches are best matched by postcritical and precritical reflections from the bottom of layers in which the velocity gradients and velocities are typical of the lower oceanic crust.

A detailed study of the amplitudes of ESP 5 was performed by Lindwall and Brocher [1986] using two-dimensional ray tracing. The crustal structures derived from one- and two-dimensional amplitude modeling agree down to the base of the crust. Lindwall and Brocher [1986], however, interpret B5 as simply a strong bubble pulse reverberation of B4 from a complex explosive source signature. In their interpretation the reflection on coincident and proximal reflection profiles at 7.0–7.3 s would either originate from the upper mantle or represent an artifact. We prefer the interpretation that these reflections represent the base of the C-M transition and thus require an additional layer to explain B5.

The thickness of the C-M transition is 5–6 km if branch B5 is included and 3.3 km if it is excluded, making the total thickness of the seismic section under the volcanic ridge between 15.8 and 18.1 km, slightly less than that inferred from previous refraction results [Furumoto *et al.*, 1968]. A subcrustal layer 5–6 km thick under the volcanic ridge and thinning under the moats with a density intermediate between the crust and the upper mantle was also required, subject to constraints

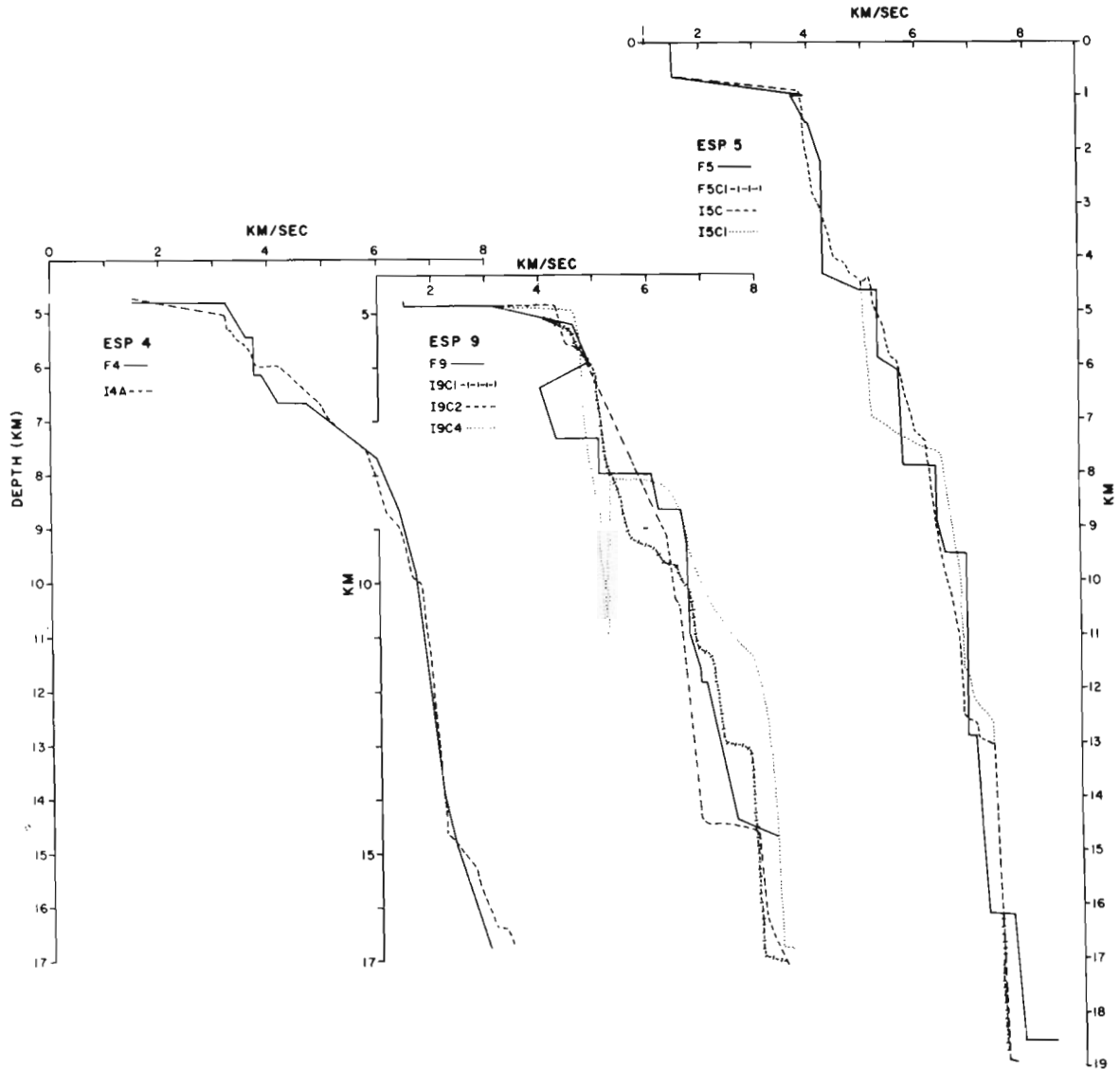


Fig. 7. Velocity-depth solutions for ESPs 4, 9, and 5. Solutions with the prefix I were obtained by τ sum inversion, and those with the prefix F were obtained by forward modeling in which travel times and amplitudes were modeled as described in the text. The negative thickness layer in solution I9C4 for ESP 9 is an artifact of the τ sum solution, caused by its inability to incorporate low-velocity zones.

imposed by the seismic data, to match the observed free air gravity anomaly in the moats and the volcanic ridge and the wavelength of the geoid anomalies (Figure 10).

Comparison to Other Seamounts and Aseismic Ridges

Elsewhere along the Hawaiian-Emperor ridge. Two seismic refraction lines shot perpendicular to the southeast and the west coasts of Hawaii [Zucca and Hill, 1980; Zucca *et al.*, 1982] reveal a gently thickening oceanic crust toward the island with a maximum depth of Moho of 18 km under Mauna Loa and 12–14 km under Kilauea. Layer 3, having a velocity of 7.1 km/s, thickens considerably under Mauna Loa but has a constant thickness under Kilauea.

Cross sections of velocity-depth solutions around Oahu compiled by Furumoto *et al.* [1968] show the C-M boundary to be 14 km deep under the moat and 19–20 km under the island. The Moho under Lanai and Maui is somewhat shallower (15–18 km), and it is also shallower under the Leeward

Islands and the seamounts toward Midway (12–14 km) [Furumoto *et al.*, 1971]. A preliminary interpretation of unreversed refraction data suggests that the Moho under Midway is located at a depth of 17.5 km below a 4-km-thick layer of 7.5- to 8.1-km/s material [Taylor, 1983]. Thus the total crustal thicknesses are comparable, and at least one of the previous refraction studies in the Hawaiian Islands suggested the existence of a lower crustal plutonic complex.

Other seamounts and aseismic ridges. Figure 11 compares the crustal structures determined at ESPs 4, 5, and 9 with results obtained at 11 other oceanic volcanic islands, seamounts, aseismic ridges, and plateaus. Although most of these results are from relatively older studies lacking the spatial resolution necessary to resolve a thin, anomalous lower crustal layer, at least three of the experiments report evidence for an anomalous C-M transition. These experiments, in the Canary Islands, the Madagascar Ridge, and the Shatsky Rise, suggest that layers having velocities between 7.0 and 7.6 km/s elsewhere overlie the upper mantle.

TABLE 1. Velocity Solutions for ESPs From Forward Modeling of Travel Times and Amplitudes

Layer No.	Two-Way Travel Time to Top, s	V_p , km/s (Top/Bottom)	Layer Thickness, km	Depth to Top of Layer, km	Observed Two-Way Travel Time, s
<i>ESP 4</i>					
1	0.00	1.5/1.5	4.79	0.00	
2	6.32	3.2/3.6	0.66	4.79	
3	6.70	3.8/3.8	0.69	5.45	
4	7.07	3.9/4.2	0.51	6.14	
5	7.32	4.7/6.0	1.06	6.65	
6	7.72	6.0/6.4	0.96	7.71	
7	8.03	6.4/6.5	0.41	8.67	
8	8.16	6.5/6.7	0.75	9.08	
9	8.39	6.7/6.9	1.75	9.83	
10	8.90	6.9/7.15	2.30	11.58	
11	9.56	7.3/7.45	1.04	13.88	
12	9.84	7.45/8.05	1.84	14.92	9.8
13	10.31			16.76	10.4
<i>ESP 9</i>					
1	0.00	1.5/1.5	4.86	0.00	
2	6.48	3.1/4.6	0.34	4.86	
3	6.66	4.6/4.9	0.69	5.20	
4	6.95	4.9/4.0	0.47	5.89	
5	7.16	4.0/4.3	0.95	6.36	
6	7.62	5.1/5.1	0.66	7.31	
7	7.88	6.1/6.2	0.67	7.97	
8	8.10	6.6/6.7	0.58	8.64	
9	8.27	6.7/6.8	1.73	9.22	
10	8.79	6.8/7.0	0.69	10.95	
11	8.99	7.0/7.0	0.22	11.64	
12	9.05	7.1/7.6	2.55	11.86	9.1
13	9.75	7.6/8.3	0.30	14.41	
14	9.82	8.3/8.5	2.37	14.71	
15	10.38			17.08	10.2
<i>ESP 5</i>					
1	0.00	1.5/1.5	0.67	0.00	
2	0.89	1.6/3.3	0.22	0.67	
3	1.08	3.3/3.9	0.13	0.89	
4	1.15	3.7/4.0	0.50	1.02	
5	1.41	4.0/4.1	0.39	1.52	
6	1.60	4.2/4.3	1.99	1.91	
7	2.73	4.3/5.0	0.30	3.90	
8	2.86	5.3/5.3	1.24	4.20	
9	3.33	5.3/5.6	0.23	5.44	
10	3.42	5.6/5.7	1.7	5.67	
11	4.04	6.3/6.4	0.98/0.67	7.37	
12A*	4.35/4.25	6.4/6.5	0.66	8.35	4.1-4.5
12B*	4.35/4.25	5.9/6.7	0.94	8.35	
13	4.55	6.8/7.0	3.36	9.01	
14	5.53	7.1/7.3	3.32	12.37	
15A*	6.45	7.7/7.9	2.34	15.69	
15B*	6.45	7.5/7.6	2.55	15.69	
16	7.05/7.13			18.03	7.0-7.3

The solutions for the sediment and uppermost crust are similar to those given by Brocher and ten Brink [1987]. V_p is compressional wave velocity.

*A and B represent alternative solutions.

The seismic refraction results from the Canary Islands, reported by Bosshard and Macfarlane [1970], are in particularly close accord with those reported in this study. At the tip of the Canary Islands chain, no higher-velocity lower crustal layer is reported, yet analogously to the Hawaiian Islands, such a layer is observed (Figure 11) 200 km behind the tip of the chain.

In a coincident multichannel seismic reflection/refraction experiment on the Shatsky Rise described by Kogan [1981],

lenticular-shaped bodies in the lower crust as well as a 7.4-km/s basal crustal layer were reported (Figure 11). As at Oahu, this high-velocity basal crustal layer pinches out to the north of the Shatsky Rise, where normal oceanic crust is observed. These results also confirm a previous refraction study of the Shatsky Rise by Den *et al.* [1969], who determined the presence of a high-velocity basal crustal layer.

Sonobuoy refraction results by Sinha *et al.* [1981] suggest a 4- to 5-km-thick high-velocity basal crustal layer beneath the Madagascar Ridge. These results were constrained by synthetic seismogram modeling of arrival amplitudes as well as travel times and are thus well constrained.

4. INTERPRETATION OF THE ANOMALOUS C-M TRANSITION AS A PLUTONIC COMPLEX

The best direct evidence in support of our interpretation of the anomalous crust-mantle transition as an intrusive (plutonic) complex at the base of the crust is the lenticular shape of reflections defined by reflections M1 and M2 in Figures 3-5. These reflections probably represent cross-sectional images of an intrusion extending away from the island. However, we cannot rule out the possibility that part of the anomalous lower crustal structure observed in CDP profiles may be caused by semibrittle faulting in the heated and weakened lower crust caused by the intrusion. For example, the disjoint steplike sections confined between reflectors M1 and M2 in line 301 (Figure 5) can be interpreted as either the termination of individual intrusions at different distances from the island or as faulting of the C-M transition. (Faulting in the sediments and at the top of the crust is observed at several locations along line 301.) We next outline the arguments in favor of the interpretation of the anomalous seismic C-M transition as related to a plutonic complex rather than to other causes and we try to investigate its properties. In section 5 we argue that the existence of an intrusive complex is consistent with a model for the volcanic history of the Hawaiian Islands.

General Evidence

The anomalous C-M transition cannot simply represent thickening of the oceanic crust with age, since this anomalous structure is not found elsewhere in our study area, nor can it represent an anomalous fracture zone crust, because of its large width (greater than 200 km). This anomalous structure cannot be caused by phase changes at the Moho, since the lithostatic pressure at the Moho is too low to account for these pressure changes. Nor can elevated temperatures at the Moho account for the anomalous crustal structure, since the diffusivity of the rock is insufficient to allow conductive heat transfer from underneath the volcano to the moats. We thus conclude that the most plausible explanation for the anomalous C-M transition zone is that it represents an intrusive complex which must be directly related to the magma upwelling and volcanism in the Hawaiian Islands.

Xenolith compositions (and CO₂ vapor inclusions within some of the xenoliths) from Hawaiian volcanoes argue for a magma chamber at a depth of 15 km or more at the end of the main shield-building and during the postcaldera collapse stages [Sen, 1983; Clague, 1987]. The lateral extent of this magma chamber must, however, be less than the radius of the overlying volcano, since mixing of lavas between adjacent volcanoes on Hawaii is not observed at these stages (D. A. Clague, personal communication, 1986). The seismically observed extent of the intrusive complex, on the other hand, is

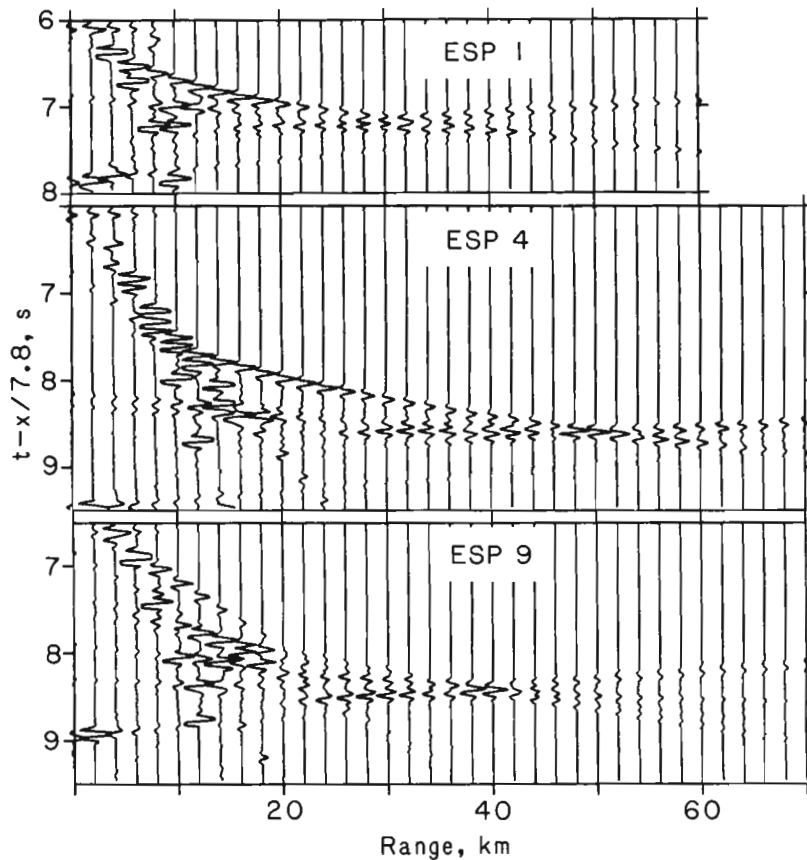


Fig. 8. Synthetic seismograms calculated for ESPs 1, 4, and 9 (at the same scale as Figure 6) using WKB theory [Chapman, 1978]. The synthetics, like the data shown in Figure 6, are plotted in true relative amplitude with no correction for geometrical spreading.

larger than the base of the volcano. We therefore prefer the interpretation that the intrusive complex under Oahu represents the accumulation of trapped upwelling magma rather than a single frozen magma chamber. Our interpretation is in accord with fractional crystallization and density models predicting that a large fraction of the upwelling magma would be underplated at the base of the crust or trapped within the crust in both the oceans (including oceanic islands) and the continents [O'Hara, 1977; Cox, 1980; Sparks *et al.*, 1980; Stolper and Walker, 1980]. These models show that a large volume of cumulates can form without requiring the existence of a large magma chamber.

Physical Properties of the Plutonic Complex

The areal extent of the anomalous C-M transition inferred to represent a subcrustal plutonic complex extends about 100 km to the north and south of Oahu (Figure 12a). The plutonic complex thickens gradually toward the island, where it attains a thickness of 3–6 km (Figure 12b). The large volume of the observed pluton suggests that the infilling magma is derived from a high melt percentage; otherwise, an unreasonably large source area is implied (D. Walker, personal communication, 1984). If so, the composition of the magma in the plutons is likely to be parental to tholeiitic basalts. Since the velocities and densities within the intrusive complex are intermediate between those of the lower crust and the upper mantle, a component more dense than tholeiitic basalt is also required. Intermediate velocities and densities would result either from

the intrusion of picritic magma into a peridotite host rock or from the presence of heavier ultramafic residue in the magma forming the plutonic complex.

The intermediate seismic velocities and densities over a depth interval of several kilometers may represent the average signature from the mixture of the frozen intrusions and the host lower crust and upper mantle rocks. This mixture forms a gradational transition between the crust and upper mantle but should also yield strongly reflective surfaces with pronounced apparent topography. The CDP reflection data do not show evidence for a strongly laminated C-M transition zone around Oahu, suggesting that the intrusive complex may not comprise individual structures of large area-to-volume ratio. Alternatively, synthetic seismograms calculated from the ophiolite models show that the fine-scale variability of the C-M transition can be obscured by narrow-band sources and random noise [Collins *et al.*, 1986].

Estimate of the Magma Supply Rate to the Plutonic Complex

The existence of the voluminous intrusive complex at the base of the crust implies that the surficial expression of volcanism constitutes only a fraction of the amount of melt generated at depth under the Hawaiian Islands. We estimate the average magma supply rate from the mantle necessary to create these intrusions as 0.1–1.0 times the rate of magma supply to Kilauea volcano (close to 10^8 m³/yr [Swanson,

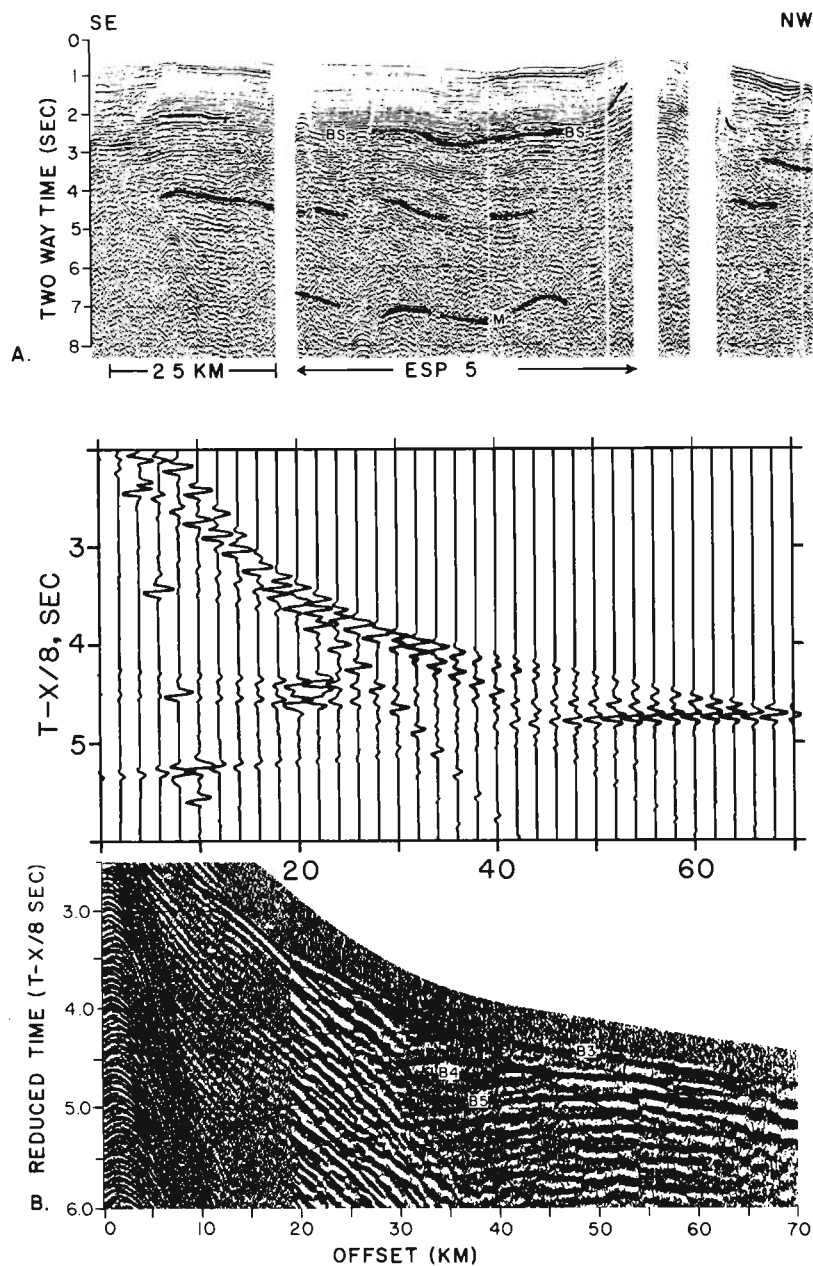


Fig. 9. (a) An interpreted display of CDP line 330 across the volcanic ridge in Kaiwi channel (location provided in Figure 2). The central section of the profile, 65 km long, parallels ESP 5. Prestack velocity filtering [Ryo, 1982] was applied to the section to remove multiples and reverberations. (b) ESP 5 plotted at a different horizontal scale using reduced travel times appropriate for 8.0 km/s. The branches marked B3–B5 represent arrivals from the lower crust and the crust-mantle transition zone. Synthetic seismograms plotted above the observed data were calculated using WKB theory [Chapman, 1978].

1972]). This estimate was made as follows: At a supply rate of 10^8 m³/yr and considering that Oahu is composed of two volcanoes, a plutonic complex $200 \times 100 \times 3$ km³ forms in 0.3 m.y. If the plutonic complex forms throughout the whole period of quiescence in volcanic activity (0.4–2.5 m.y. for the Hawaiian Islands [Clague and Dalrymple, 1987]), the average rate of magma supply necessary to fill the pluton during this period is 0.1–1.0 times the supply rate to Kilauea. The average supply rate would be even smaller if the plutonic complex is instead composed of smaller but more numerous intrusions into the country rock rather than a solid 3-km-thick intrusion.

Flexure and the Plutonic Complex

On the basis of a preliminary interpretation of a limited portion of the data set analyzed here, Watts *et al.* [1985] showed two possible structures for the crust under Oahu. The first crustal structure maintained a uniform thickness as it flexed under the island load in accord with the proposed structure from earlier flexure studies [Watts and Cochran, 1974; Watts, 1978], but it required a dense core under the center of the island to fit the observed gravity and geoid. The second structure did not require a dense core; however, the

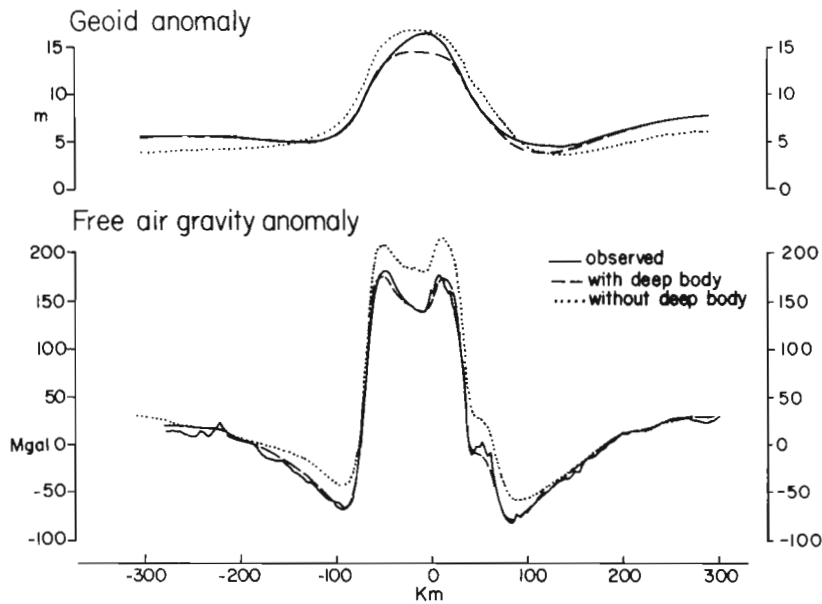


Fig. 10. Comparison of observed and calculated gravity and geoid profiles based on a density model constrained by the seismic data (Figure 12b) and common velocity-density relationships [Christensen and Salisbury, 1975; Manghni and Woollard, 1968]. The effect of the subcrustal plutonic complex on the gravity field is emphasized by the comparison with two calculated models, one which includes the plutonic complex (dashed line) and another which replaces it with upper mantle material (dotted line). In particular, the gravity field over the bathymetric moats and the wavelength of the geoid anomaly could not be matched without the contribution from the plutonic complex. The discrepancy between amplitudes of the observed and calculated geoid (with the subcrustal plutonic complex) above the volcanic ridge arises from the passage of the satellite track above the SW edge of Oahu's landmass (westward of ESP 5). The observed free air gravity data were collected aboard the R/V *Kana Keoki* during the collection of lines 301 and 314 and ESP 5, and the observed geoid anomaly was derived by subtracting a Goddard Earth Model (GEM) 10 earth model (degree and order 12) from a descending track of Seasat.

crust thinned progressively toward the center of the island. The large-aperture CDP profiles and the solutions for ESPs 5 and 9 show crustal thinning north of the Oahu; hence, they better support the second structure.

The plutonic complex in our cross section (Figure 12b) represents a buried load on the lithosphere. This load is believed to exert only a small effect on lithospheric flexure, since it replaced both the lower density oceanic crust and the higher-density upper mantle. Similarly, simple calculations of the cooling rate of a partially molten intrusion, 3 km thick, suggest that the thermal effect of pluton emplacement on the flexure of the lithosphere is negligible since this intrusion cools to temperatures below the plastic deformation regime (at geological strain rates [Brace and Kohlstedt, 1980]) after less than 10^5 years.

5. TEMPORAL VARIATIONS IN THE FLEXURAL STRESS FIELD: A MODEL FOR THE VOLCANIC HISTORY

As the oceanic lithosphere is loaded and depressed by a linear volcano chain as illustrated in Figure 13, horizontal flexural stresses develop in response to the load. In this section we investigate the possible role these flexural stresses play in the cessation of volcanism and the initiation of subcrustal intrusive activity at the postcaldera stage and on the resumption of volcanism in the posterosional stage. In the appendix we outline the formulation of elastic plate stresses, from which it is evident that the magnitude of the stresses is dependent on the curvature of the flexed lithosphere and is linearly dependent on the value of Young's modulus and on the depth within the elastic plate at which the stresses are calculated.

From Figure 13 it is clear that large variations in the curvature of the flexural lithosphere along the trend of the island chain lead to significant temporal variations in the horizontal stresses associated with the flexure.

Flexural Stress Model

A map view of flexural plane stresses at the depth of the Moho calculated for an elastic plate loaded by a line load comparable in size to the Hawaiian chain is shown in Figure 14. The volcanic load along the chain is uniform in height except for a 40-km-long segment next to the active tip of the chain, where it is 30–60% larger. This load distribution is a close approximation to the relative size of Hawaiian volcanoes because of the substantially higher (47%) relative density of subaerial loads compared to subaqueous loads. The elastic plate thickness (T_e) used to calculate Figure 14 changed linearly from 30 km at the tip of the line load and at the flexural arches which surround the line load to 23 km under the line load to the left of stage 4. This linear change in plate thickness (i.e., rigidity) is in accord with *ten Brink and Watts's* [1985] independent analysis, which indicated a decrease in rigidity along the island chain due to the transient reheating of the lithosphere.

Profiles of the horizontal stresses at the Moho under the center of the volcanic line (along the top of the map) show significant changes in the sign and magnitude of the stresses under the volcanic line (Figure 14). These stress profiles also represent the temporal changes in the stress field of an individual volcano as it migrates from the tip of the chain to the middle of the chain (or alternatively, as the active tip of the

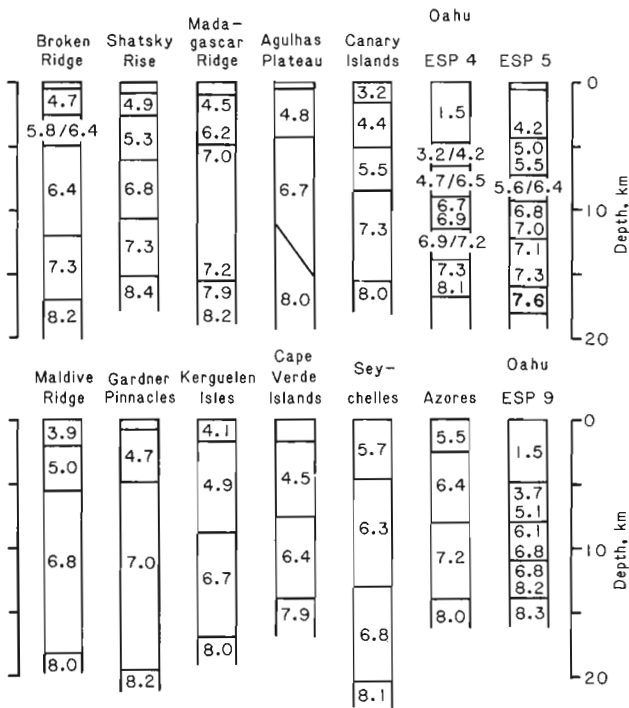


Fig. 11. Comparison of velocity-depth solutions for 11 oceanic plateaus and aseismic ridges with results from this study. The data sources for this compilation include Broken Ridge [Francis and Raitt, 1967], Shatsky Rise [Kogan, 1981], Madagascar Ridge [Sinha et al., 1981], Agulhas Plateau [Barret, 1977], Canary Islands [Bossard and Macfarlane, 1970], Maldive Ridge [Francis and Shor, 1966], Gardner Pinnacles [Hales and Nation, 1973], Cape Verde Islands [Weigel et al., 1982], Kerguelen Isles [Recq and Charvis, 1986], Seychelles [Francis and Shor, 1966], and the Azores [Hirn et al., 1980].

line load propagates forward, leaving the volcano behind). Because of the variation of curvature of the lithosphere along the chain (Figure 13), the deviatoric stresses perpendicular to the volcanic chain (y direction) are compressive beginning at about 110 km ahead of the tip of the line load (stage 1), reach maximum compression at a distance of 80 km behind the load tip (stage 3), and remain compressive along the line load. Figure 13 shows that the deviatoric stresses parallel to the direction of the line load (x direction), on the other hand, change from tensional near stage 1, reach maximum compression 80 km behind the tip (stage 3), and then decrease significantly further down the chain until they again become slightly tensional about 190 km behind the point of maximum compression (stage 4). Bearing in mind that flexural stages 1–4 correspond to the relative locations of each volcano at its nascent, shield-building, postcaldera, and posterosional stages, we next correlate these stages to the magmatic and volcanic history of the Hawaiian Islands.

Formation of the Subcrustal Plutonic Complex

The formation of the subcrustal plutonic complex can be most readily understood by considering the depth dependence of the pressure and stress under a Hawaiian volcano at stage 3, corresponding to the postcaldera stage. Figure 15 shows the lithostatic pressure in the unloaded lithosphere, a hypothetical magma pressure profile (assuming an interconnected conduit throughout the lithosphere), and the smaller of the pair of stresses (σ_x).

Magma can flow through conduits in the upper part of the

lithosphere and erupt as long as the horizontal compressive flexural stresses are smaller than the magmatic pressure, but the conduits are blocked when the horizontal compressive stresses exceed the magma pressure (represented by the hatched area in Figure 15). Once the conduits are blocked at the base of the crust, the magma will propagate by hydraulic fracturing in a plane normal to the least compressive stress direction [e.g., Weertman, 1971]. Since the horizontal flexural stresses exceed those of the vertical load (the lithostatic stress in Figure 15), the least compressive stress at the Moho is vertical; thus a horizontal intrusion will form at or just below the lower crust. The intrusion may propagate parallel to the flexed surface by utilizing the anisotropic structure of the layered mafic and ultramafic cumulates at the crust-mantle (C-M) boundary. This plutonic complex starts forming during the postcaldera collapse stage after the volcano has attained its full size and the compressive flexural stresses have reached their maximum magnitude (state 3). Because the magnitudes of the flexural stresses are smaller below a smaller volcano, the development of a plutonic complex may be delayed for smaller volcanoes until the magma pressure decreases.

The lateral extent of the plutonic complex depends on both the pressure head at the tip of the pluton and the regional stress field. The outer limit of the pluton propagation is defined by the change at the Moho level of the flexural stress field from horizontal deviatoric compression to tension at a distance of 80–100 km from the center of the island (about $\pi/4$ of the flexural wavelength). At this range, intrusions can no longer propagate horizontally as the least compressive stress becomes horizontal in Figure 14. This limiting range for horizontal pluton formation closely matches the distance north and south of Oahu at which the anomalous C-M transition is observable.

Thermally induced stresses and strains tend to reinforce the blockage of vertical conduits and the growth of a plutonic complex (represented in Figure 16a by the curve for 0.1 m.y. after emplacement). However, these thermal stresses decrease rapidly as the temperature perturbation decays in the rock surrounding the pluton and hence allow renewed eruptions in the posterosional stage 4 (2 m.y. after emplacement; Figure 16a). The magnitude of the calculated stresses in this figure probably represents the upper limit of induced thermal stresses, since the plutonic complex may well be composed of thin lateral intrusions into a 3-km-thick host rock rather than the modeled 3-km-thick pluton. Furthermore, if convective heat transfer occurs within the intrusion, thermal stresses will be larger after 0.1 m.y. but smaller than shown after 2 m.y.

Posterosional Eruptions

In view of the hot spot hypothesis, which suggests that a thermal plume exists under the tip of the island chain, the resumption of volcanism well behind the tip presents a problem. Both thermal and mechanical models have been proposed to account for the posterosional volcanism observed along the Hawaiian Islands chain and other midplate volcanic chains. Jackson and Wright [1970, p. 427] proposed a flexural explanation for the orientation of the dikes on Oahu: They suggested that

the change (indicated by tide gauge data) from subsidence to uplift (on Oahu) may have provided the energy at depth to initiate ... the nephelinitic basalts of the Honolulu Series. Moore calculates that the elastic arch passed nearly at right-angles to

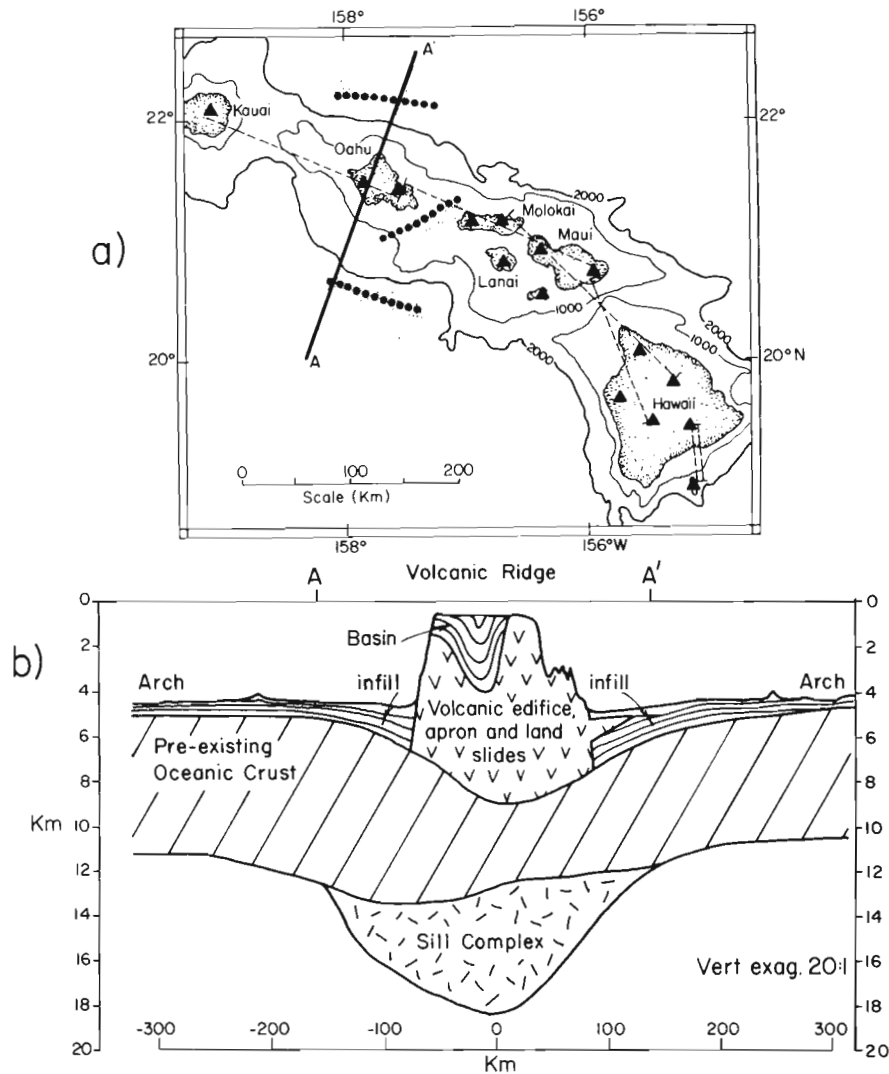


Fig. 12. (a) Map view of the locations where the existence of a plutonic complex is inferred from the seismic data; shaded areas are inferred from CDP data, and solid circles from ESPs. Solid triangles indicate volcanic centers along the Hawaiian chain, and dashed lines the distances between pairs of volcanoes which were simultaneously active in their shield and posterosional stages. Double dashed lines indicate the distance between volcanoes in their nascent and shield-building stages. (b) A cross section through points A and A' (heavy line on the map in Figure 12a) showing the crustal structure based on the analysis of the seismic reflection and refraction data presented in this paper and in the work by U. S. ten Brink and T. M. Brocher (Multichannel seismic evidence for variations in crustal thickness across the Molokai Fracture Zone in the mid-Pacific, submitted to *Journal of Geophysical Research*, 1987).

the Hawaiian chain, which would account for the general cross-alignment of Honolulu vents. ...

In contrast, *Gurriet* [1987] proposed a thermal origin for alkalic posterosional lavas in which low percentages of partial melt are produced in the lower lithosphere by reheating of the lithosphere by the hot spot. This thermal mechanism does not explain how these magmas are erupted. *Nakamura and Fumii* [1987] proposed that thermal stresses associated with the main stage of shield volcanism are responsible for later cracking of the lithosphere accompanied by posterosional volcanism.

Our flexural model explains the initiation of posterosional eruptions at a constant distance from the contemporaneous active shield [*Clague and Dalrymple*, 1987] by the change in the direction of the least compressive stress from vertical to

horizontal, which occurs at a constant distance behind the active shield (the distance between stages 2 and 4; Figure 13). Since the least compressive stress direction determines the orientation of the intrusions, posterosional dikes and vents again develop instead of horizontally oriented plutons.

The flexural model predicts that dike orientation in the posterosional stage 4 will be perpendicular to the volcanic chain, because at this stage the least compressive stress axis is parallel to the volcanic chain. This dike orientation is observed on Oahu where rift systems connecting the posterosional vents of the Koolau shield lie perpendicular to the trend of the island chain [*Jackson and Wright*, 1970]. Furthermore, since the posterosional dike system of the Honolulu Series on Koolau is also perpendicular to the earlier Koolau rift, active at the shield-building stage, this dike orientation cannot be the result of exploiting a preexisting zone of weakness. A similar

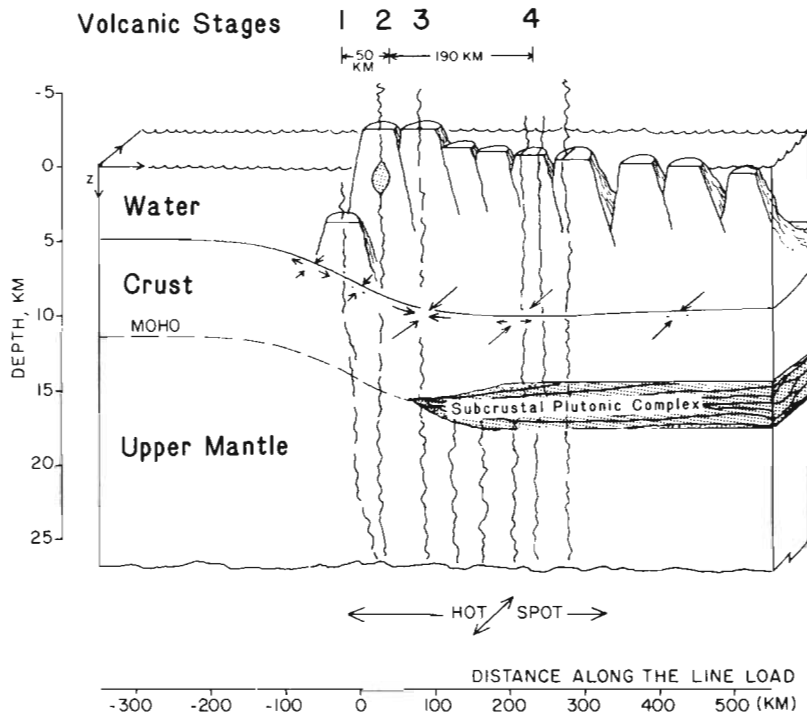


Fig. 13. A schematic depth cross section along the Hawaiian Islands chain. The figure can be taken as either a time series of one volcano or a snapshot of a series of volcanoes. The deflection of the seafloor is calculated using a two-dimensional finite difference elastic plate model (W. R. Buck, personal communication, 1986). Arrows along the seafloor deflection curve indicate qualitatively the sign and magnitude of the horizontal components of the deviatoric stress field underneath the center of this chain. The distance from the active stage to the nascent volcano and the posterosional stage are 50 km and 190 km, respectively. The plutonic complex is believed to develop during or after the postcaldera stage and before the posterosional stage. The arrows surrounding the hot spot mark the spatial extent of upwelling magma in the middle part of the lithosphere.

cross-ridge orientation of the posterosional vents is observed on Kauai, where the vents trend NNE-SSW to N-S [Macdonald and Abbott, 1970].

Orientation of Main Rifts

Experimental modeling [Fiske and Jackson, 1972] and the existence of rift zones on Loihi seamount [Moore et al., 1982] indicate that the orientation of rifts of the shield-building stage in Hawaiian volcanoes is determined early in the development of a new volcano. The orientations of the principal flexural stress axes in our model are sensitive to the exact shape of the load at the tip of the line load (Figure 14). In particular, at the tip of the line load (stage 1) the least compressive stress is horizontal and subparallel to the direction of steepest slope. Hence rifts in nascent volcanoes are expected to be oriented along-strike the steepest slopes of the nearest large volcano. This orientation was observed by Fiske and Jackson [1972]; however, these authors attributed the rift orientations of volcanoes which developed in the vicinity of existing volcanoes to local gravitational stresses in the volcanic pile. Our flexural model suggests that the preferred orientation of rifts is also found in the underlying crust.

The orientations of the rifts in isolated shields [Fiske and Jackson, 1972] are not adequately explained by the flexural stress field model, because the magnitude of flexural stresses tens of kilometers ahead of the tip of the line load is small (Figure 14). These orientations have been qualitatively ex-

plained as the result of regional stresses encompassing the entire plate [Jackson et al., 1972; Nakamura, 1977].

6. DISCUSSION

The proposed flexural model, in which the temporal change in the flexural stress field under the volcano modulate the sequence of volcanic activity, explains the formation and width of the plutonic complex as well as the location and orientation of posterosional eruptions and many rifts along the Hawaiian chain. In particular, the formation of a subcrustal plutonic complex is explained as an integral part of the volcanic and magmatic sequence of the Hawaiian Islands (Figure 13). Since the load modeled is a simplification of the actual distribution of the Hawaiian volcanoes (i.e., some considerable volcanic gaps occur in the island chain, the volume of the volcanoes is not uniform, and they are not arranged on a perfect straight line), deviations from the calculated stress field of Figure 14 are expected. This may, in turn, cause small deviations from the steady state sequence of volcanic and magmatic activity.

Periodic changes in the buoyancy of the upwelling magma and compositional changes leading to viscosity variations in the magma may also play a role in determining the volcanic sequence. For example, the early alkalic lavas from Loihi have a high gas content, which may provide the mechanism for breaking up new conduits through the lithosphere [Moore and Clague, 1981]. However, temporal variations in magma pressure due to compositional variations are probably too gradual

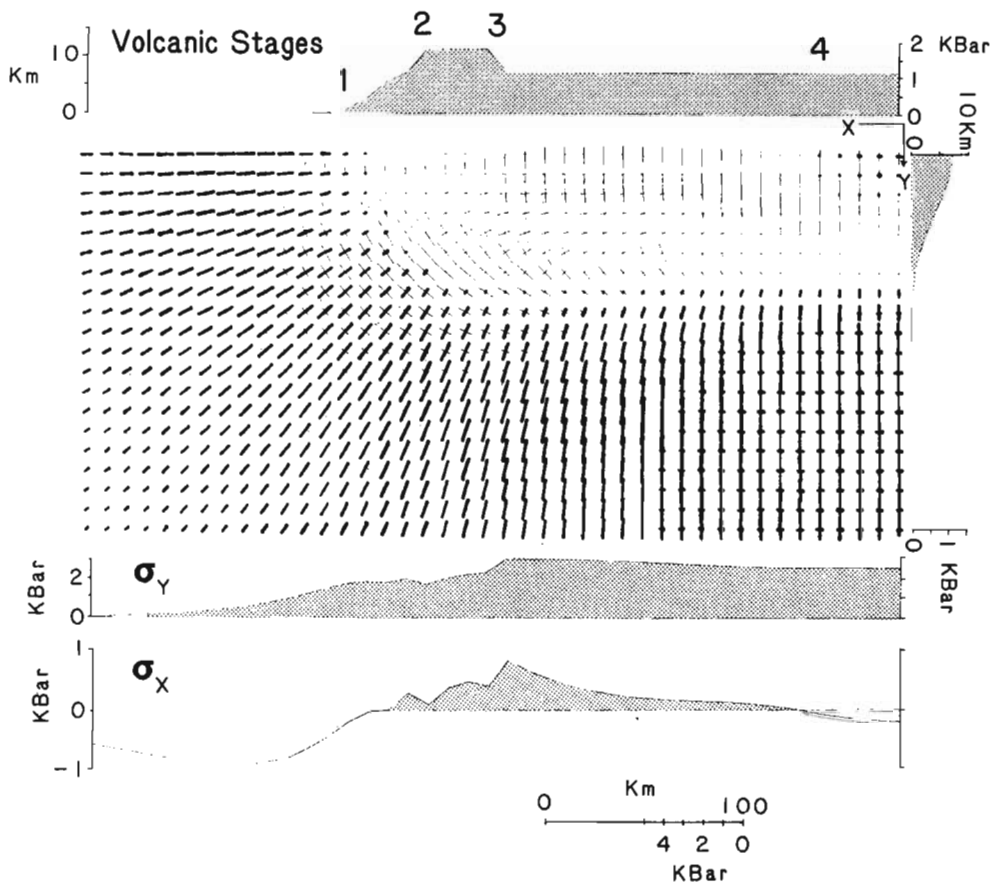


Fig. 14. Map view of the modeled plane stress field in a thin elastic plate due to loading by a line load comparable in size to the Hawaiian Islands. The directions of the bars represent the directions of the maximum and minimum horizontal stresses, the length of the bars is scaled in proportion to their magnitude at the Moho level, and the crossing point between two perpendicular bars gives the location of these stresses in a map view. Heavy bars represent both deviatoric tension and the least compressive stress, because the vertical load is subtracted from the magnitude of the plane stresses. Light bars represent horizontal compression in excess of the lithostatic. The top row of the map is located under the centerline of a symmetric load; the shape of the load (along the top row and left column) is shown in two orthogonal profiles above and to the right of the map. Profiles of the two orthogonal horizontal stresses under the center of the line load are plotted under the map with similar distance scale. (Positive stress values indicate deviatoric compression and are shaded; negative stress values show deviatoric tension.) As described in the text, stages 1-4 correspond to the position of Hawaiian volcanoes at the four volcanic stages (Figure 1).

to produce the observed variations in the eruption rates and cannot explain the constant distance between shield and post-erosional volcanism. Viscosity variations between picritic and nephelinitic basalts are insignificant if variations in volatile content are ignored [McKenzie, 1985].

Stress Field Versus Other Possible Controls on the Formation of the Plutonic Complex

The flexural stress model for subcrustal pluton formation does not exclude other mechanisms offered by petrological models [O'Hara, 1977; Cox, 1980; Sparks *et al.*, 1980; Stolper and Walker, 1980]. In particular, a density filter which is imposed by the crust on the upwelling magma [Stolper and Walker, 1980; Sparks *et al.*, 1980] may also generate a plutonic complex which will grow from the inception of volcanism. To test the influence of the stress field on the formation of the pluton, one should look for a crustal pluton under Loihi, Kilauea, and Mauna Loa, the currently active volcanoes at the tip of the line load. The existence of a large pluton under these volcanoes will indicate that pluton formation is primarily controlled by other mechanisms (e.g., the

density filter) and not by the flexural stress field (the opposite conclusion is not necessarily true).

There is currently no geophysical evidence for a lower crustal pluton or an anomalous crust-mantle transition underneath the youngest Hawaiian volcanoes. Previous seismic refraction and tomographic studies, however, had poorer resolution than the data presented here [Ellsworth and Koyanagi, 1977; Zucca *et al.*, 1982; etc.]. The existence of a plutonic complex might also be tested with heat flow data. Figure 16b shows the predicted heat flow anomaly from a 3-km-thick horizontal intrusion which is emplaced instantaneously at the base of the crust. The surface heat flow perturbation grows rapidly in time to 55% of the regional heat flow at 0.7 m.y. after sill emplacement.

Application of the Model to Other Linear Chains

Volcanic and magmatic histories similar to that of the Hawaiian Islands are observed in other island chains and groups such as the Samoan, Canary, and Comoro islands [Staudigel *et al.*, 1984]. The eruptive sequence of the Canary Islands is rather similar to that of the Hawaiian Islands [Schmincke,

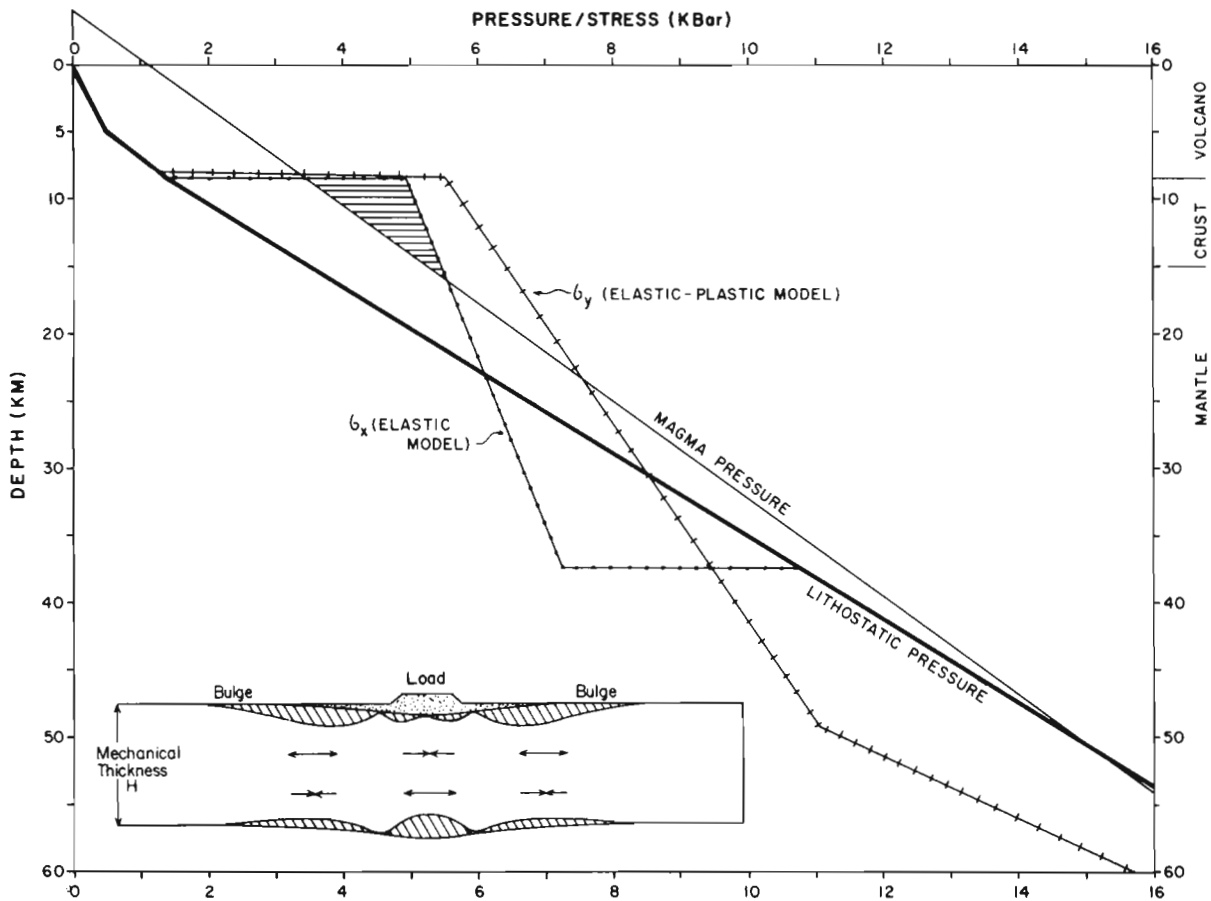


Fig. 15. The depth dependence of pressures and stresses under a hypothetical Hawaiian volcano during its postcaldera stage (stage 3). Heavy line indicates the initial (before loading) lithostatic stress condition of the lithosphere; light line shows the magma pressure in a volcano extending 4 km above sea level assuming interconnected conduit throughout the lithosphere and no viscous dissipation. Densities of mantle rock and magma are 3300 kg/m^3 and 2800 kg/m^3 . Dotted line represents the minimum horizontal stress profile (σ_x) as a function of depth, calculated by a two-dimensional elastic model (appendix). The plutonic complex is located at and below the depth at which the minimum horizontal stress is larger than the magma pressure (hatched area). At this depth the least compressive stress is vertical (the lithostatic pressure). Crossed line indicates the maximum horizontal stresses (σ_y), calculated from an elastic-plastic model [Bodine *et al.*, 1981], 10^5 years after load emplacement. Whereas in the simple elastic plate model no failure is predicted, a more realistic rheology of the oceanic lithosphere is incorporated into the elastic-plastic model. The region of deviatoric horizontal tension in the later model extends to depths larger than the equivalent elastic thickness (T_e) of the plate. Note that the σ_y profile shown here is calculated by a different model than that used to obtain the profile of σ_x and that used to generate the stresses shown in Figure 14 and thus is not directly comparable to these profiles. The inset shows a schematic cross section [from Bodine *et al.*, 1981] of the deflection of the "mechanical" lithosphere under a seamount load. Arrows pointing outward indicate deviatoric tensile stresses, and those pointing inward show compressive stresses in the elastic core of the lithosphere. The hatched areas indicate the extent of brittle (top) and ductile (bottom) failure due to these stresses.

1982]. In particular, a posterosional stage is also found in the Canary Islands after a period of quiescence as long as 9 m.y. The eruptions at that stage are perpendicular to the orientations of the dikes which erupted in the shield stage. The Canary Islands are characterized by magmatism of highly peralkaline felsic compositions during the waning shield stages. Furthermore, seismic evidence [Bosshard and Macfarlane, 1970] suggests that a high-velocity lower crustal layer develops only behind the tip of the chain.

Because of the similarities in the volcanic sequence and seismic structures between Hawaii and the Canary Islands it is tempting to conclude that the flexural stress field modulates the sequence of activity in the Canary Islands and that a subcrustal pluton exists there, too. However, there are significant differences between the shape and continuity of the Canary and the Hawaiian loads, their rate of propagation,

and their underlying lithospheres. These differences, though, if reflected in dissimilarities in the details of the eruptive sequence between the two island groups, could be exploited to study the differences in the rheology and state of stress between the lithospheres in these two locations.

Implications for the Lithosphere and Hot Spots

Although the "hot spot" hypothesis [Wilson, 1963; Morgan, 1972] is widely accepted as the explanation for the creation of the Hawaiian Islands chain, competing mechanisms such as the various propagating fracture models [Green, 1971; Jackson *et al.*, 1972; Solomon and Sleep, 1974; Walcott, 1976; Turcotte and Oxburgh, 1978] have also been proposed. In these models, magmas are released to the surface by stress-induced cracking and destruction of the integrity of the lithosphere.

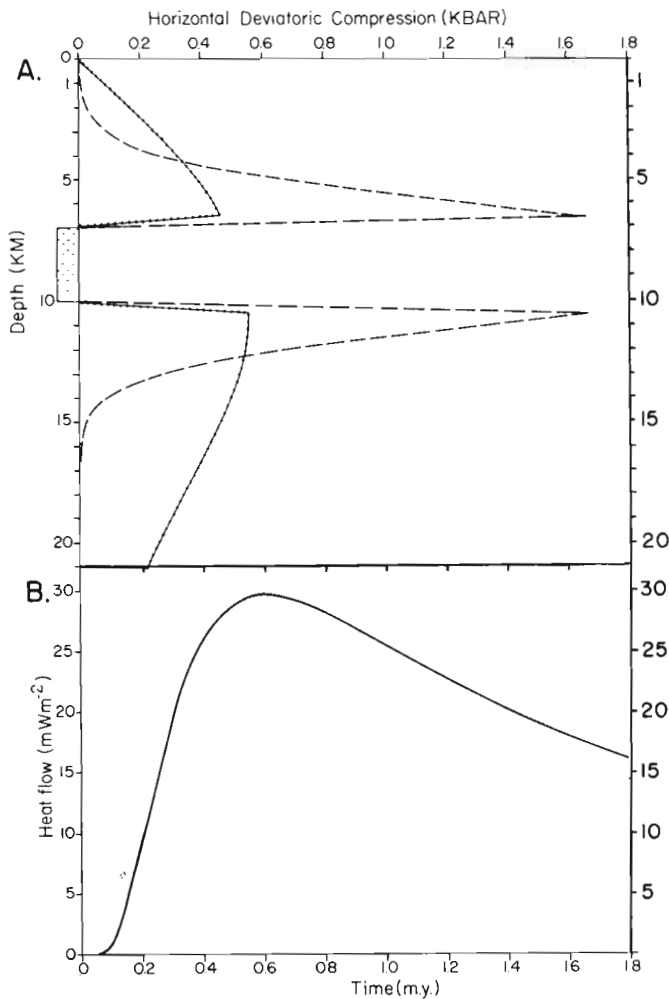


Fig. 16. (a) The calculated horizontal thermal stresses above and below a 3-km-thick sill at 0.1 m.y. (dashed line) and 2 m.y. (dotted line) after the emplacement of the sill at the base of the oceanic crust (location of the sill is marked by crosses). An initial magma temperature of 1100°C and a 20% melt are assumed [Wright *et al.*, 1976]. The additional horizontal compressive stresses and extensional vertical strains are proportional to the magnitude of the thermal perturbation [Boley and Weiner, 1960]. The calculation is simplified by using one-dimensional temperature perturbation [Carslaw and Jaeger, 1959, p. 62], which is a close approximation for the region away from the edges of the sill. (b) The calculated surface heat flow as a function of time after sill emplacement. Neglect of the convective heat transfer within the sill means that the heat flow perturbation may occur at earlier times than calculated here. The conductivity used to calculate the heat flow ($0.775 \text{ W m}^{-1} \text{ K}^{-1}$) and the average heat flow value for the area surrounding Hawaii before reheating, $52 \pm 2 \text{ mW m}^{-2}$, are from Von Herzen *et al.* [1982].

The fundamental assumption in our proposed flexural stress model is that the elastic plate is continuous under the volcanic chain. If instead the plate is broken under the island chain and the two half plates are free to move against each other, there are no horizontal deviatoric stresses under the volcanic chain. Acceptance of the flexural stress field model for Hawaiian volcanism therefore results in rejecting the different models of propagating fracture, and vice versa.

In the model presented here, the stress field in the upper part of the lithosphere modulates the eruption or subcrustal accumulation of magma upwelling along a segment about 300

km long between the tip of the volcanic chain and the volcano at the end of its posterosional stage (Figure 13). In other words, magma upwelling in the lower lithosphere is not limited to the small area under the active shield volcano. Therefore the thermal perturbation in the asthenosphere and the lower lithosphere must be quite wide, too, in accord with Detrick and Crough's [1978] interpretation of the broad Hawaiian swell (approximately 1200 km wide). Further support for a broad zone of magmatic upwelling is provided by observations of simultaneous (i.e., within the last 500 years) eruptions of Canary [Schmincke, 1982] and Samoan volcanoes [Natland, 1980] along a 400-km-long segment.

According to the flexural model the distal part of the hot spot produces the posterosional volcanism. This could explain the strongly alkaline character of the posterosional eruptions (small percent of partial melt; see Figure 1) as opposed to the mildly alkaline to tholeiitic character (higher percent of partial melt) of the main shield volcanism. By itself, however, the flexural model provides no explanation for the geochemistry of the posterosional lavas.

The flexural stresses created in an elastic plate by a surface load are coupled: If deviatoric compression occurs in the upper part of the mechanically rigid lithosphere, then deviatoric tension must occur in the lower part of the plate (Figure 15), and vice versa. Hence the area under deviatoric tension at the base of the "mechanical" lithosphere is defined by the area of compression in the upper part of the plate (Figure 14). This area begins at the tip of the line load, continues under the island chain, and stretches 80–100 km on each side of the center of the volcanic chain. A two-dimensional elastic-plastic plate model (Figure 15) shows that the deviatoric tensional stresses in this area reach their maxima at depths of 45–50 km. Outside this area, horizontal stresses are tensile in the upper part of the lithosphere and therefore more compressive in the bottom part of the mechanical lithosphere. (This model considers the rheological properties of the lithosphere and therefore represents the stress distribution with depth more realistically than the simple elastic model.) Since horizontal deviatoric tension facilitates magma upwelling, magma ascending through the middle part of the lithosphere preferentially rises in the area undergoing deviatoric tension. According to a magma transport theory [Weertman, 1971], tensile stresses must exist at the lower part of the elastic plate in order to cause the nucleation of bottom cracks into the plate (assuming equal magma and lithostatic pressure at the bottom of the plate). Hence the flexural stress field may help "channel" magma from a wider and deeper source zone, which does not have to be centered directly under the tip of the island chain, into a narrower (roughly $300 \times 200 \text{ km}^2$) area under the island chain (Figure 13).

It may not be a coincidence that the depth range in which channeling of magma is predicted by the model is also the range of deep volcanic tremors [Eaton and Murata, 1960; Klein, 1982]. According to the elastic-plastic plate model (Figure 15) the lithosphere is highly ductile at depths greater than 60 km and is not expected to generate earthquakes. The distribution of earthquake epicenters under the island of Hawaii contains a gap at a depth of 20–25 km [Klein, 1982], which corresponds to the depth of the neutral surface of the elastic-plastic plate model (Figure 15). Thus the 60-km-deep earthquakes under Hawaii in those portions of the plate which are capable of storing stress may be related to stress release due to either magma migration or bending of the plate.

7. SUMMARY

Evidence from a variety of multichannel seismic methods indicates that an anomalous C-M transition exists under the volcanic ridge and the flanking moats near Oahu, Hawaii. Large-aperture CDP reflection profiles delineate an anomalous crustal thickness, show variable relief on the inferred C-M boundary, and indicate the presence of two (or more) reflections, M1 and M2, in the lower crust and upper mantle under the moats. Velocity-depth solutions inferred from three coincident ESPs indicate the presence of thickened C-M transition with velocities intermediate between those of layer 3 and the upper mantle under Oahu. The anomalous seismic transition zone probably represents ascending parental picritic magmas (including their ultramafic components) which were trapped at the base of the oceanic crust (subcrustal plutonic complex). Although thickened oceanic crusts under aseismic ridges and seamounts were known from previous refraction studies, the seismic data presented here, in particular, the wide-aperture reflection data (0.3–7.5 km), provide for the first time evidence of the nature and structure of this intrusive complex. The existence of such voluminous intrusions at the base of the crust implies that the surficial expression of volcanism constitutes only a fraction of the amount of melt generated at depth under the Hawaiian Islands.

The model presented in this paper suggests an interaction between the upwelling magma from a hot spot source and the stress field created by the products of this upwelling (i.e., the volcanoes), which determines the characteristic eruption history of Hawaiian volcanoes. While a wide, deep-seated source in the vicinity of the tip of the island chain supplies the buoyant magma for eruptions or subcrustal intrusions, the details of the volcanic and magmatic activities are governed to a large extent by the flexural stress field which develops in response to loading by the volcanic chain. A similar analysis of the stress field for other volcanic chains or groups over "moving" or "stationary" hot spots may help predict the sequence and details of their volcanic activity and may reveal details about the rheology of the underlying lithosphere. Similarly, the analysis of the changing stress field with time in orogenic belts, island arcs, and rift shoulders may explain the onset and termination of volcanic and intrusive activity in these regions.

APPENDIX: PRINCIPAL STRESSES
IN A THIN ELASTIC PLATE

The deflection ω of an elastic plate under the load of a volcanic chain is found by solving the following equation with the set of assumptions known as the "thin plate approximation" [Timoshenko and Woinowsky-Krieger, 1959]:

$$\nabla^2(D\nabla^2\omega) = P(x, y) + k\omega$$

and the boundary conditions (for simply supported edges) at $x, y \rightarrow \infty$:

$$\omega = 0 \quad \nabla^2\omega = 0$$

where D is the rigidity, P the load, and k the restoring force. Prior to loading, the state of stress in the lithosphere is assumed to be hydrostatic. The equation was solved numerically by a two-dimensional finite difference method with reflective boundaries along $x, y = 0$ (W. R. Buck, personal communication, 1986). The results were compared to a solution obtained using the Fourier transform of the above equation (J.

R. Cochran, personal communication, 1986) for a continuous plate with uniform rigidity and simply supported edges. Following Timoshenko and Woinowsky-Krieger [1959], the strains in a thin plate undergoing a small deflection are

$$\epsilon_n = z/r_n \quad \epsilon_\tau = z/r_\tau$$

where r_n and r_τ are the curvatures of the plate in two horizontal orthogonal axes and z is the distance from the neutral surface. Using Hooke's law, the corresponding stresses at level z within the plate are

$$\sigma_n = Ez/(1 - \nu^2)[1/r_n + \nu(1/r_\tau)]$$

$$\sigma_\tau = Ez/(1 - \nu^2)[1/r_\tau + \nu(1/r_n)]$$

where E is Young's modulus and ν is Poisson's ratio. If the deflections of the plate are very small, the curvature of the neutral surface in the direction n can be approximated as

$$1/r_n = -\partial/\partial n(\partial\omega/\partial n)$$

The operator $\partial/\partial n$ is expressed in the x, y coordinate system as

$$\partial/\partial n = \partial/\partial x \cos \alpha + \partial/\partial y \sin \alpha$$

where α is the angle between x and n . Hence the curvatures in directions n and τ in x, y coordinates are

$$1/r_n = 1/r_x \cos 2\alpha - 1/r_{xy} \sin 2\alpha + 1/r_y \sin 2\alpha$$

$$1/r_\tau = 1/r_x \sin 2\alpha + 1/r_{xy} \sin 2\alpha + 1/r_y \cos 2\alpha$$

where $1/r_x = -\partial^2\omega/\partial x^2$, $1/r_y = -\partial^2\omega/\partial y^2$, and $1/r_{xy} = \partial^2\omega/\partial x \partial y$. The curvatures of the surface are maximum or minimum when the derivatives of these equations equal zero, from which the direction n of maximum curvature is found:

$$\tan 2\alpha = -(2/r_{xy})/(1/r_x - 1/r_y)$$

The vertical load $P(x, y)$ was subtracted from the maximum and minimum horizontal stresses in Figure 14 in order to show the least compressive stress in the plate (heavy bars).

Acknowledgments. We thank P. Buhl, J. Alsop, and the technicians and operators of the Multichannel Seismic group at Lamont-Doherty Geological Observatory for their assistance in the processing of the seismic data. We thank D. Clague for his permission to duplicate Figure 1 prior to its publication and for providing preprints of his work. We thank R. Buck, J. Cochran, R. Hobbs, J. Luetgert, and E. Vera for the use of their computer programs. Discussions with D. Clague, M. Bieniek, and D. Lindwall were helpful. J. Diebold, D. Fornari, D. Hill, J. McCarthy, J. Mutter, D. Walker, and A. Watts carefully reviewed earlier drafts of this manuscript and offered helpful suggestions. The critical reviews of R. Detrick and an anonymous reviewer improved the manuscript. Financial support by NSF grants OCE85-14073 (LDGO) and OCE84-43349 (WHOI) and by the U.S. Geological Survey (for T.M.B.) is acknowledged. Lamont-Doherty Geological Observatory Contribution 4164.

REFERENCES

- Barret, D. M., Agulhas Plateau off southern Africa: A geophysical study, *Geo. Soc. Am. Bull.*, 88, 749–763, 1977.
 Bodine, J. H., M. S. Steckler, and A. B. Watts, Observations of flexure and the rheology of the oceanic lithosphere, *J. Geophys. Res.*, 86, 3695–3707, 1981.
 Boley, B. A., and J. H. Weiner, *Theory of Thermal Stresses*, 586 pp., John Wiley, New York, 1960.
 Bosshard, E., and D. J. Macfarlane, Crustal structure of the western Canary Islands from seismic refraction and gravity data, *J. Geophys. Res.*, 75, 4901–4918, 1970.

- Brace, W. F., and D. L. Kohlstedt, Limits on lithospheric stress imposed by laboratory experiments, *J. Geophys. Res.*, **85**, 6248–6252, 1980.
- Brocher, T. M., and U. S. ten Brink, Variations in oceanic layer 2 elastic velocities near Hawaii and their correlation to lithospheric flexure, *J. Geophys. Res.*, **92**, 2647–2661, 1987.
- Buhl, P., J. B. Diebold, and P. L. Stoffa, Array length magnification through the use of multiple sources and receiving arrays, *Geophysics*, **47**, 311–315, 1982.
- Carlsaw, H. S., and J. C. Jaeger, *Conduction of Heat in Solids*, Oxford University Press, New York, 1959.
- Chapman, C. H., A new method for computing synthetic seismograms, *Geophys. J. R. Astron. Soc.*, **54**, 481–518, 1978.
- Chase, T. E., H. W. Menard, and J. Mammerickx, Bathymetry of the North Pacific, charts 7 and 8, Scripps Inst. of Oceanogr., San Diego, Calif., 1970.
- Christensen, N. I., and M. H. Salisbury, Structure and constitution of the lower oceanic crust, *Rev. Geophys.*, **13**, 57–86, 1975.
- Clague, D. A., Hawaii alkaline volcanism, in *Alkaline Igneous Rocks*, edited by J. G. Fitton and B. G. J. Upton, Geological Society of London, London, in press, 1987.
- Clague, D. A., and G. B. Dalrymple, The Hawaiian-Emperor volcanic chain, I, Geological evolution, *U.S. Geol. Surv. Prof. Pap.*, **1350**, 5–54, 1987.
- Collins, J. A., T. M. Brocher, and J. F. Karson, Two-dimensional seismic reflection modeling of the oceanic crust/mantle transition in the Bay of Islands ophiolite complex, *J. Geophys. Res.*, **91**, 12,520–12,538, 1986.
- Cox, K. G., A model for flood basalt volcanism, *J. Petrol.*, **21**, 629–650, 1980.
- Den, N., et al., Seismic refraction measurements in the northwest Pacific basin, *J. Geophys. Res.*, **74**, 1421–1434, 1969.
- Detrick, R. S., and S. T. Crough, Island subsidence, hot spots, and lithospheric thinning, *J. Geophys. Res.*, **83**, 1236–1244, 1978.
- Diebold, J. B., and P. L. Stoffa, The travel-time equation, tau-p mapping and inversion of common midpoint data, *Geophysics*, **46**, 238–254, 1981.
- Eaton, J. P., and K. J. Murata, How volcanoes grow, *Science*, **132**, 925–938, 1960.
- Ellsworth, W. L., and R. Y. Koyanagi, Three-dimensional crust and mantle structure of Kilauea volcano, Hawaii, *J. Geophys. Res.*, **82**, 5379–5394, 1977.
- Fiske, R. S., and E. D. Jackson, Orientation and growth of Hawaiian volcanic rifts: The effect of regional structure and gravitational stresses, *Proc. R. Soc. London, Ser. A*, **329**, 299–326, 1972.
- Francis, T. J. G., and R. W. Raitt, Seismic refraction measurements in the southern Indian Ocean, *J. Geophys. Res.*, **72**, 3015–3041, 1967.
- Francis, T. J. G., and G. G. Shor, Seismic refraction measurements in the northwest Indian Ocean, *J. Geophys. Res.*, **71**, 427–449, 1966.
- Furumoto, A. S., G. P. Woollard, J. F. Campbell, and D. M. Hussong, Variation in the thickness of the crust in the Hawaiian Archipelago, in *The Crust and Upper Mantle of the Pacific Area*, *Geophys. Monogr. Ser.*, vol. 12, edited by L. Knopoff, C. L. Drake, and P. J. Hart, pp. 94–111, AGU, Washington, D. C., 1968.
- Furumoto, A. S., J. F. Campbell, and D. M. Hussong, Seismic refraction surveys along the Hawaiian ridge, Kauai to Midway, *Bull. Seismol. Soc. Am.*, **61**, 147–166, 1971.
- Green, D. H., Composition of basaltic magmas as indicators of origin: Application to oceanic volcanism, *Philos. Trans. R. Soc. London, Ser. A*, **268**, 707–725, 1971.
- Guirret, P., A thermal model for the origin of post-erosional alkalic lava, Hawaii, *Earth Planet. Sci. Lett.*, **82**, 153–158, 1987.
- Hales, A. L., and J. B. Nation, A seismic refraction study in the southern Indian Ocean, *Bull. Seismol. Soc. Am.*, **63**, 1951–1966, 1973.
- Hirn, A., H. Haessler, P. Hoang Trong, G. Wittlinger, and L. A. Mendes Victor, Aftershock sequence of the January 1st, 1980, earthquake and present day tectonics of the Azores, *Geophys. Res. Lett.*, **7**, 501–504, 1980.
- Jackson, E. D., and T. L. Wright, Xenoliths in the Honolulu Volcanic Series, Hawaii, *J. Petrol.*, **11**, 405–430, 1970.
- Jackson, E. D., E. A. Silver, and G. B. Dalrymple, Hawaiian-Emperor chain and its relation to Cenozoic Circumpacific tectonics, *Geol. Soc. Am. Bull.*, **83**, 601–618, 1972.
- Klein, F. W., Earthquakes at Loihi submarine volcano and the Hawaiian hot spot, *J. Geophys. Res.*, **87**, 7719–7726, 1982.
- Kogan, L. I., Crustal structure of the Shatsky Rise of the northwest Pacific, from deep seismic reflection profiling, *Dokl. Acad. Sci. USSR Earth Sci. Sect.*, Engl. Transl., **258**, 25–30, 1981.
- Lindwall, D. A., and T. M. Brocher, Crustal structure under the Hawaiian Islands, *Eos Trans. AGU*, **67**, 1083, 1986.
- Macdonald, G. A., and A. T. Abbott, *Volcanoes in the Sea, the Geology of Hawaii*, University of Hawaii Press, Honolulu, 1970.
- Manghnani, M. H., and G. P. Woollard, Elastic wave velocities in Hawaiian rocks at pressures to ten kilobars, in *The Crust and Upper Mantle of the Pacific Area*, *Geophys. Monogr. Ser.*, vol. 12, edited by L. Knopoff, C. L. Drake, and P. J. Hart, pp. 501–516, AGU, Washington, D. C., 1968.
- McKenzie, D., The extraction of magma from the crust and mantle, *Earth Planet. Sci. Lett.*, **74**, 81–91, 1985.
- Moore, J. C., and D. A. Clague, Loihi seamount lavas: Volatile contents, *Eos Trans. AGU*, **62**, 1083, 1981.
- Moore, J. C., D. A. Clague, and W. R. Normark, Diverse basalt types from Loihi seamount, Hawaii, *Geology*, **10**, 88–92, 1982.
- Morgan, W. J., Deep mantle convection plume and plate motions, *Am. Assoc. Pet. Geol. Bull.*, **56**, 203–312, 1972.
- Nakamura, K., Volcanoes as possible indicators of tectonic stress orientation—Principle and proposal, *J. Volcanol. Geotherm. Res.*, **2**, 1–16, 1977.
- Nakamura, K., and N. Fujii, Hawaiian volcanism: Result of heating and subsequent cooling of a fast moving plate over a fixed hot spot, paper presented at Hawaii Symposium on How Volcanoes Work, U.S. Geol. Surv., Hilo, Hawaii, Jan. 19–26, 1987.
- Natland, J. H., The progression of volcanism in the Samoan linear volcanic chain, *Am. J. Sci.*, **280-A**, 709–735, 1980.
- NAT Study Group, North Atlantic Transect: A wide-aperture, two-ship multichannel seismic investigation of the oceanic crust, *J. Geophys. Res.*, **90**, 10,321–10,341, 1985.
- O'Hara, M. J., Geochemical evolution during fractional crystallisation of a periodically refilled magma chamber, *Nature*, **266**, 503–507, 1977.
- Requ, M., and P. Charvis, A seismic refraction survey in the Kerguelen Isles, southern Indian Ocean, *Geophys. J. R. Astron. Soc.*, **84**, 529–559, 1986.
- Ryo, J. V., Decomposition (DECOM) approach applied to wave field analysis with seismic reflection records, *Geophysics*, **47**, 869–884, 1982.
- Schmincke, H.-U., Volcanic and chemical evolution of the Canary Islands, in *Geology of the Northwest African Margin*, edited by U. von Rad et al., pp. 273–306, Springer-Verlag, New York, 1982.
- Sen, G., A petrologic model for the constitution of the upper mantle and crust of the Koolau shield, Oahu, Hawaii, and Hawaiian magmatism, *Earth Planet. Sci. Lett.*, **62**, 215–228, 1983.
- Sinha, M. C., K. E. Loudon, and B. Parsons, The crustal structure of the Madagascar Ridge, *Geophys. J. R. Astron. Soc.*, **66**, 351–377, 1981.
- Solomon, S. C., and N. H. Sleep, Some simple physical models for absolute plate motions, *J. Geophys. Res.*, **79**, 2557–2567, 1974.
- Sparks, R. S. J., P. Meyer, and H. Sigurdsson, Density variation amongst mid-ocean ridge basalts: Implications for magma mixing and the scarcity of primitive lavas, *Earth Planet. Sci. Lett.*, **46**, 419–430, 1980.
- Staudigel, H., A. Zindler, S. R. Hart, T. Leslie, C.-Y. Chen, and D. Clague, The isotope systematics of a juvenile intraplate volcano: Pb, Nd, and Sr isotope ratios of basalts from Loihi seamount, Hawaii, *Earth Planet. Sci. Lett.*, **69**, 13–29, 1984.
- Stoffa, P. L., and P. Buhl, Two-ship multichannel seismic experiments for deep crustal studies: Expanded spread and constant offset profiles, *J. Geophys. Res.*, **84**, 7645–7660, 1979.
- Stoffa, P. L., P. Buhl, J. B. Diebold, and F. Wenzel, Direct mapping of seismic data to the domain of intercept time and ray parameter—A plane-wave decomposition, *Geophysics*, **46**, 255–267, 1981.
- Stolper, E., and D. Walker, Melt density and the average composition of basalt, *Contrib. Mineral. Petrol.*, **74**, 7–12, 1980.
- Swanson, D. A., Magma supply rate of Kilauea volcano, 1952–1971, *Science*, **1975**, 169–170, 1972.
- Taylor, D. W. A., The structure of the crust and upper mantle near Midway Island, M.Sc. thesis, New Mexico State Univ., Las Cruces, 1983.
- ten Brink, U.S., Lithospheric flexure and Hawaiian volcanism: A multichannel seismic perspective, Ph.D. thesis, Columbia Univ., New York, 1986.
- ten Brink, U. S., and A. B. Watts, Seismic stratigraphy of the flexural moat flanking the Hawaiian Islands, *Nature*, **317**, 421–424, 1985.

- Timoshenko, S., and S. Woinowsky-Krieger, *Theory of Plates and Shells*, McGraw-Hill, New York, 1959.
- Tsai, C. J., An analysis leading to the reduction of scattered noise on deep marine seismic records, *Geophysics*, 49, 17–26, 1984.
- Turcotte, D. L., and E. R. Oxburgh, Intra-plate volcanism, *Philos. Trans. R. Soc. London, Ser. A*, 288, 561–579, 1978.
- Von Herzen, R. P., R. S. Detrick, S. T. Crough, D. Epp, and U. Fenn, Thermal origin of the Hawaiian swell: Heat flow evidence and thermal models, *J. Geophys. Res.*, 87, 6711–6724, 1982.
- Walcott, R. I., Flexure of the lithosphere at Hawaii, *Tectonophysics*, 9, 435–446, 1970.
- Walcott, R. I., Lithospheric flexure, analysis of gravity anomalies, and the propagation of seamount chains, in *The Geophysics of the Pacific Ocean Basin and Its Margin*, *Geophys. Monogr. Ser.*, vol. 19, edited by G. H. Sutton, M. H. Manghnani, and R. Moberly, pp. 431–438, AGU, Washington, D. C., 1976.
- Watts, A. B., An analysis of isostasy in the world's oceans, 1, Hawaiian-Emperor seamount chain, *J. Geophys. Res.*, 83, 5989–6004, 1978.
- Watts, A. B., and J. R. Cochran, Gravity anomalies and flexure of the lithosphere along the Hawaiian-Emperor seamount chain, *Geophys. J. R. Astron. Soc.*, 38, 119–141, 1974.
- Watts, A. B., U. S. ten Brink, P. Buhl, and T. M. Brocher, A multi-channel seismic study of lithospheric flexure across the Hawaiian-Emperor seamount chain, *Nature*, 315, 105–111, 1985.
- Weertman, J., Theory of water-filled crevasses in glaciers applied to vertical magma transport beneath oceanic ridges, *J. Geophys. Res.*, 76, 1171–1183, 1971.
- Weigel, W., G. Wissmann, and F. Goldflam, Deep seismic structures (Mauritania and central Morocco), in *Geology of the Northwest African Margin*, edited by U. von Rad et al., pp. 132–159, Springer-Verlag, New York, 1982.
- Wilson, J. T., A possible origin of the Hawaiian Islands, *Can. J. Phys.*, 41, 863–870, 1963.
- Wright, T. L., D. L. Peck, and H. R. Shaw, Kilauea lava lakes: Natural laboratories for study of cooling, crystallization, and differentiation of basaltic magma, in *The Geophysics of the Pacific Ocean Basin and Its Margin*, *Geophys. Monogr. Ser.*, vol. 19, edited by G. H. Sutton, M. H. Manghnani, and R. Moberly, pp. 375–390, AGU, Washington, D. C., 1976.
- Zucca, J. J., and D. P. Hill, Crustal structure of the southeast flank of the Kilauea volcano, Hawaii, from seismic refraction measurements, *Bull. Seismol. Soc. Am.*, 70, 1149–1159, 1980.
- Zucca, J. J., D. P. Hill, and R. L. Kovach, Crustal structure of Mauna Loa volcano, Hawaii, from seismic refraction and gravity data, *Bull. Seismol. Soc. Am.*, 72, 1535–1550, 1982.

T. M. Brocher, U.S. Geological Survey, 345 Middlefield Road, MS 977, Menlo Park, CA 94025.

U. S. ten Brink, Department of Geophysics, Stanford University, Stanford, CA 94305.

(Received October 21, 1986;
revised May 5, 1987;
accepted May 16, 1987.)